AD-A146 938 WHITE-LIGHT OPTICAL INFORMATION PROCESSING AND HOLOGRAPHY(U) PENNSYLVANIA STATE UNIVUUNIVERSITY PARK DEPT OF ELECTRICAL ENGINEERING F T YU 22 JUN 84 1/1

UNCLASSIFIED AFOSR-TR-84-0889 AFOSR-83-0140 F/G 14/5 NL

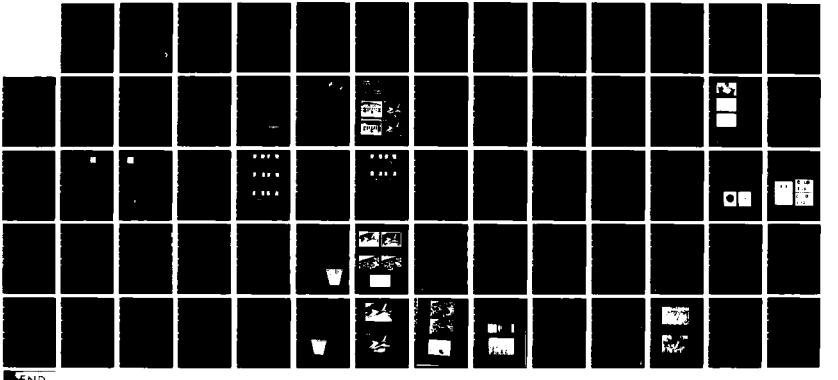

END

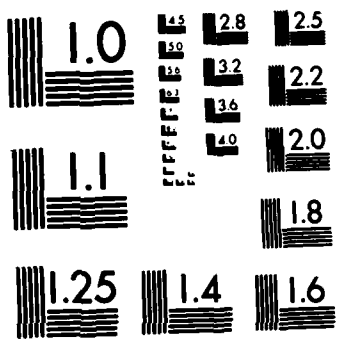

(2)

# White-Light Optical Information Processing and Holography



by

F. T. S. Yu
(Principal Investigator)

Electrical Engineering Department
The Pennsylvania State University
University Park, Pennsylvania 16802

Prepared for:

AFOSR/NE

Building 410
Bolling Air Force Base
Washington, D.C. 20332

Attention: Dr. Robert W. Carter, Jr.

AFOSR Annual Report on
Contract AFOSR 83-0140

Period Covered (March 15, 1983 - March 14, 1984)

Date: June 22, 1984

UNCLASSIFIED
SECURITY CLASSIFICATION OF THIS PAGE (When Data Entered)

| REPORT DOCUMENTATION PAGE | READ INSTRUCTIONS BEFORE COMPLETING FORM |
|---|---|
| 1. REPORT NUMBER: AFOSR-TR- 84-0889 | 2. GOVT ACCESSION NO.: AD-A146 938 |
| 3. RECIPIENT'S CATALOG NUMBER | |
| 4. TITLE (and Subtitle): White-Light Optical Processing and Holography | 5. TYPE OF REPORT & PERIOD COVERED: Annual Report, March 15, 1983 - March 14, 1984 |
| | 6. PERFORMING ORG. REPORT NUMBER |
| 7. AUTHOR(s): Francis T. S. Yu | 8. CONTRACT OR GRANT NUMBER(s): AFOSR - 83 - 0140 |
| 9. PERFORMING ORGANIZATION NAME AND ADDRESS: Electrical Engineering Department, The Pennsylvania State University, University Park, PA 16802 | 10. PROGRAM ELEMENT, PROJECT, TASK AREA & WORK UNIT NUMBERS: 61102F, 2305/B1 |
| 11. CONTROLLING OFFICE NAME AND ADDRESS: AFOSR/NE, Building 410, Bolling Air Force Base, Washington, DC 20332 | 12. REPORT DATE: June 21, 1984 |
| | 13. NUMBER OF PAGES |
| 14. MONITORING AGENCY NAME & ADDRESS (If different from Controlling Office): Dr. Robert W. Carter, Jr., AFOSR/NE, Bolling Air Force Base, Washington, DC 20332 | 15. SECURITY CLASS. (of this report): Unclassified |
| | 15a. DECLASSIFICATION DOWNGRADING SCHEDULE |

16. DISTRIBUTION STATEMENT (of this Report)

Approved for public release; distribution unlimited.

17. DISTRIBUTION STATEMENT (of the abstract entered in Block 20, if different from Report)

18. SUPPLEMENTARY NOTES

19. KEY WORDS (Continue on reverse side if necessary and identify by block number)

White-Light Optical Processing, Image Deblurring, Source Encoding, Signal Sampling, Coherence Measurement, Noise Performance, Pseudocolor Encoding.

20. ABSTRACT (Continue on reverse side if necessary and identify by block number)

~~During the~~ third year (FY'83) a great deal of progress has been made on the white-light optical information processing and holography research program. ~~In this period, we have~~ completed ~~the~~ work ~~of~~ a broad band color image deblurring and ~~have extended~~ this technique to the restoration of 2-D out-of-focused color photographic images. ~~We have also~~ developed a new technique of white-light density pseudocolor encoder for three primary colors. This white-light pseudocolor encoder is very cost effective and

DD FORM 1 JAN 73 1473 EDITION OF 1 NOV 65 IS OBSOLETE

UNCLASSIFIED
SECURITY CLASSIFICATION OF THIS PAGE (When Data Entered)

20. ABSTRACT (Continued)

offers a high image resolution, which would be an excellent alternation for the digital counterpart. We have also in this period conducted a measuring technique for the degree of coherence in the Fourier plane of the grating-based white-light signal processor. We have shown that high degree of coherence is achievable with a signal sampling grating at the input plane. Thus the white-light technique is capable of processing the information in complex amplitude and it is very suitable for color signal processing. In this phase of research we have also studied the effect of coherence due to source encoding, signal sampling and spectral band filtering, as applied to the white-light signal processing. The effect of source encoding is to relax the constraints of a physical light source, and the effect of the signal sampling is to improve the degree of temporal coherence at the Fourier plane. Thus the signal can be carried out by a broad spectral filter. In this period, we have investigated the noise performance of a white-light signal processor. The noise performance under the temporally incoherent illumination is quantitatively analyzed. We have shown that the output signal-to-noise ratio improves considerably with the increasing the spectral bandwidth of the light source employed. In addition, we have also evaluated a dual-beam encoding technique for color holographic construction. The color hologram image can be easily reproduced by a white-light processing technique. This encoding technique would offer the simplicity of color hologram generation without utilizing a reference beam. In brief, we have shown again the versatility of the proposed white-light processing technique.

## Table of Contents

## I. Introduction

In the past year, we have accomplished several major research works on white-light optical information processing area. Our research programs were consistent with our AFOSR grant, for which in part have been published in various refereed journals and conference proceedings, and have been presented to several scientific conferences (e.g., OSA, SPIE). Sample copies of these articles are included in this annual report in the subsequent sections, to provide a concise documentation of our research program. In the following sections, we shall give an overview of our research work done in the period from March 15, 1983 to March 14, 1984. We will detail some of those accomplished works. A list of publications resulting from AFOSR's support is included at the end of this report.

## II. Summary and Overview

Although optical signal processing has the unique abilities of (1) complex amplitude processing, (2) parallel processing capability, (3) high resolution, (4) speed, and (5) color, however the lack of versatility, stringent processing environment, artifact noise, costly light sources, etc., those are the major impediments for the slow emerging as possible alternation to the digital counterpart. Nevertheless, there are techniques for optical signal processing that can successfully compete against the electronic and digital systems. One of those techniques would be the white-light signal processing technique. The advantages of the white-light signal processing are: (1) It eliminates the coherent artifact, (2) the white-light source is generally inexpensive, (3) the processing environment is rather relaxed, (4) the white-light processor is easy and economical to maintain, and (5) the processor is very suitable for color signal processing.

We have, in the past few years, developed a grating based white-light optical signal processing technique [1,2] to processing the optical signal in complex amplitude. We have illustrated that this white-light processing technique is capable of suppressing the coherent artifact as an incoherent processor [3] and at the same time it can process the information in complex amplitude as a coherent processor [4]. In an article [5], we have shown, that smeared-photographic-image can be deblurred with white-light processing technique, since the white-light sources possess all the visible color wavelengths, it is particularly suitable for color image processing: For example, the color image deblurring [6], archival storage of color film [7], pseudocolor encoding [8] and others. We have also developed a source encoding concept [9] in which the inability of an extended white-light source may be alleviated. That is, for a processing operation, a source encoding technique may be generated to provide a specific spatial coherence function that is suitable for the processing, e.g., the image subtraction with encoded incoherent source [10,11]. In other words, a broad spatial coherence function may not be needed for certain optical processing operations. It is possible, however, to obtain a reduced spatial coherence function for a specific processing operation by spatially encoding the light source. We have also extended the incoherent image subtraction technique for color images [11,12]. As compared with the results obtained with a coherent source, we see that, the results obtained with incoherent and white-light techniques offer a higher image quality than those obtained with coherent processsing technique [13].

We have, also in the past two years, investigated the coherence requirement for this white-light optical processing technique [14]. These basic optical processing operations are evaluated. We have shown that for

the linear image deblurring problem, the spatial coherence requirement is dependent upon the source size, smeared length, and spatial frequency of the grating. While for image subtraction problems, the coherence requirement is dependent upon the ratio of slit size to the spacing of the slits of a source encoding mask, the slit size, the spectral bandwidth of the light source and the separation of the input object transparencies. For correlation detection [15], the requirement for temporal coherence strongly depends on the spatial frequency and the spatial extension of the target (i.e., space bandwidth product). However, the spatial coherence requirement depends only on the extension of the target.

We have also formulated an apparent transfer function of this proposed white-light optical processing system [16]. Although these formulas show that the apparent transfer function is dependent upon the degree of spatial and temporal coherence, there is actually more variability in the spatial coherence. We note that the obtained formulas may also be used as a criterion in the selection of source size and spectral bandwidth of an incoherent light source. Thus a specific optical information processing operation can be carried out with an incoherent source.

We have also in this period evaluated the (white-light transmission) rainbow holographic aberrations and its bandwidth requirements [17]. We have shown the conditions for the elimination of the five primary rainbow holographic aberrations. These conditions may be useful for the application of obtaining a high quality rainbow hologram image. In terms of bandwidth requirement, we have shown that the bandwidth requirement for a rainbow holographic construction is usually several orders lower than that of a conventional holographic process, hence a lower resolution recording medium can generally be used.

We have also conducted a research on the detection of phase object variation through color encoding with encoded extended incoherent sources [18]. This technique provides fine detail of the object phase variation between fringes, including both the positive and negative phase variations.

In the following sections, we shall highlight some of the research done during the past year effort on white-light signal processing.

2.1 Broad Spectral Band Color Image Deblurring (Section III)

In the past twelve months, we have conducted a broad spectral band color image deblurring [19]. The technique utilizes a fan-shape broad spectral band deblurring filter to compensate the scale variation of the smeared Fourier spectra. This technique is particularly suitable for linear smeared color image deblurring.

2.2 Noise Performance

In this period, we have also quantitatively analyzed the noise performance for a white-light signal processor. The analysis is broken down into two major parts; the effects due to temporal coherence and due to spatial coherence. We have completed the noise performance due to the temporally partially coherent illumination, for which a paper is submitted for publication [20].

2.3 Pseudocolor Encoding with Three Primary Colors (Section IV).

We have also in this period developed a white-light density pseudocolor encoder for three primary colors [21]. The advantages of this technique are; it is very cost effective and offers a high image resolution, as compared with the digital technique.

2.4 Partial Coherent Measurement (Section V).

We have, in this phase, accomplished a coherent measurement for our white-light optical signal processor [22]. The results show that the

degree of coherence in this Fourier plane increases as the spatial frequency of the sampling grating increases. However, the improvement in coherence is somewhat more effective in the direction perpendicular to light dispersion. Since the white-light processor is capable of processing complex signal with entire spectral band of the light source, it is suitable for color signal processing.

2.5 Restoration of Out-of-Focused Color Image (Section VI).

In this period, we have also extended the color image deblurring to 2-D out-of-focused color photographic images [23]. Final results of this restoration technique have been obtained.

2.6 Source Encoding, Sampling and Spectral Band Filtering (Section VII).

We have also in the past year developed a general concept on source encoding, signal sampling and spectral band filtering for a white-light processor [24]. A similar paper was also presented to the 10th International Optical Computing Conference at M.I.T. on April 6-8 [25].

2.7 Advances in White-Light Optical Signal Processing (Section VIII).

We have also in this period reported a paper on the recent advances in white-light to the proceedings on Optical Information Processing Conference II, NASA Langley Research Center [26].

2.8 Remarks

We have also, in this period, investigated the real-time and computer controllable processing capability as applied to white-light signal processing. We are also currently developing a computer generated filter algorithm for our white-light signal processor. Interesting results would be surfaced in the near future. In short, the white-light signal processing research program, supported by AFOSR, is conducted extremely well as proposed. As it can be seen, several significant results have been

documented in open literatures available for the interested technical and research staffs, for example, as listed in Section III to VIII.

2.9 Future Research

Our aim in the following years is toward the following goals:

1. The synthesize a low cost computer controllable white-light pseudocolor encoder.

2. To carry out the white-light programmable pseudocolor encoder for multispectral band satellite pictures, x-ray transparencies, scanning electron micrograph, etc.

3. Measurement of the noise performance of the white-light signal processor.

4. To develop a real-time programmable processing capability for the white-light signal processing technique.

5. To carry out various real-time signal processing applications.

6. To develop a real-time color signal processing capability.

7. Provide experimental demonstrations and applications of the principles and processing operation that we proposed.

8. To develop techniques of synthesizing a broad spectral band complex matched filter for the white-light processing system.

9. To develop a computer generated spatial filters program that is suitable for broad spectral band white-light processing.

10. To develop a technique of utilizing real-time magneto-optics spatial light modulator for filter synthesis, as applied to white-light.

11. Improve the resolution, system performance, and signal-to-noise ratio of the proposed system.

12. To develop a generalized source encoding technique for the proposed white-light processor.

13. To develop a sun-light processing capability.

14. Evaluate the merits, constraints, and limitations of the proposed system.

15. To develop techniques of generating and reconstructing hologram philosophies of the US Air Force and DOD needs.

The modern tactical and strategic Air Force engagement scenarios assume rapid, effective, secure, independent processing and communication among many ground and airborne stations. We believe that the proposed work will have a profound and direct effort on Air Force processing system as well as provide substantial "fall out" benefit in such areas as radar, sonar, tracking, targeting, surveillance, inspection, and many others.

## 2.10 References


1. F. T. S. Yu, "A New Technique of Incoherent Complex Signal Detection," Opt. Commun., 27, 23 (1978).

2. F. T. S. Yu, "Restoration of Smeared Photographic Image by Incoherent Optical Processing," Appl. Opt., 17, 3571 (1978).

3. F. T. S. Yu and H. T. Chao, "Experiments of White-Light Processing Utilizing a Diffraction Grating Method," Optik, 56, 423 (1980).

4. L. J. Cutrona et. al., "Optical Data Processing and Filtering Systems," IRE Trans. Inform. Theory, IT-6, 386 (1960).

5. S. L. Zhuang, T. H. Chao and F. T. S. Yu, "Smeared Photographic Image Restoration with White-Light Optical Processing," Opt. Lett., 6, 109 (1981).

6. F. T. S. Yu, S. L. Zhuang and T. H. Chao, "Color-Photographic-Image Deblurring by White-Light Processing Technique," J. of Opt., 13, 57 (1982).

7. F. T. S. Yu, "White-Light Processing Technique for Archival Storage of Color Films," Appl. Opt., 19, 2457 (1980).

8. F. T. S. Yu, S. L. Zhuang, T. H. Chao and M. S. Dymek, "Real-Time White-Light Spatial Frequency and Density Pseudocolor Encoder," Appl. Opt., 19, 2986 (1980).

9. F. T. S. Yu, S. L. Zhuang and S. T. Wu, "Source Encoding for Partially Coherent Optical Processing," Appl. Phy. B 27, 99

(1982).

10. S. T. Wu and F. T. S. Yu, "Source Encoding for Image Subtraction," Opt. Lett., 6, 452 (1981).

11. F. T. S. Yu and S. T. Wu, "Color Image Subtraction with Encoded Extended Incoherent Source," J. Opt. (in press).

12. F. T. S. Yu, "Optical Image Subtraction," Photonics (in press).

13. F. T. S. Yu and J. L. Horner, "Optical Processing of Photographic Images," Opt. Eng., 20, 666 (1981).

14. S. L. Zhuang and F. T. S. Yu, "Coherence Requirement for Partially Coherent Optical Information Processing," Appl. Opt., 21, 2587 (1982).

15. F. T. S. Yu, Y. W. Zhang and S. L. Zhuang, "Coherence Requirement for Partially Coherent Correlation Detection," Appl. Phys. B 30, 23 (1983).

16. S. L. Zhuang and F. T. S. Yu, "Apparent Transfer Function for Partially Coherent Optical Information Processing," Appl. Phys., B 28, 359 (1982).

17. Y. W. Zhang, W. G. Zhu and F. T. S. Yu, "Rainbow Holographic Aberrations and the Bandwidth Requirements," Appl. Opt., 7, 581 (1982).

18. S. T. Wu and F. T. S. Yu, "Visualization of Color Coded Phase Object Variation with Incoherent Optical Processing Technique," J. Opt. 13, 111 (1982).

19. T. H. Chao, S. L. Zhuang, S. Z. Mao and F. T. S. Yu, "Broad Spectral Band Color Image Deblurring," Appl. Opt., 22, 1439 (1983).

20. F. T. S. Yu, S. L. Zhuang and K. S. Shaik, "Noise Performance of a White-Light Optical Signal Processor: Part I. Temporally Partially Coherent Illumination," J. Opt. Soc. Am. A., 1, 489 (1984).

21. F. T. S. Yu, X. X. Chen and T. H. Chao, "White-Light Density Pseudocolor Encoding with Three Primary Colors," J. Opt., 15, 55 (1984).

22. F. T. S. Yu, F. K. Hsu and T. H. Chao, "Coherence Measurement of a Grating-Based White-Light Optical Signal Processor," Appl. Opt., 23, 333 (1984).

23. S. J. Lu and F. T. S. Yu, "Restoration of Out-of-Focused Color Photographic Images," Opt. Commun., 46, 278 (1983).

24. F. T. S. Yu, "Source Encoding, Signal Sampling and Spectral Band

Filtering for Partially Coherent Optical Signal Processing," J. Opt., 14, 173 (1983).

25. F. T. S. Yu, "Source Encoding, Signal Sampling and Filtering for White-Light Signal Processing," Proc. 10th International Optical Computing Conference, April 6-8 (1983).

26. F. T. S. Yu, Advances in White-Light Optical Signal Processing," Proc. on Optical Information Processing Conference II, NASA CP-2303 Conference Publication, pp. 53-69, August (1983).

# SECTION III

## Broad Spectral Band Color Image Deblurring

Reprinted from Applied Optics, Vol. 22, page 1439, May 15, 1983


# Broad spectral band color image deblurring

T. H. Chao, S. L. Zhuang, S. Z. Mao, and F. T. S. Yu

A broadband white-light processing technique for smeared color photographic image deblurring is described. The technique utilizes a diffraction grating method to disperse the smeared image spectra in the Fourier plane so that the entire spectral band of the white-light source can be utilized for the deblurring. In this paper the technique of synthesizing a fan-shape type complex deblurring filter to accommodate wavelength variation is presented. Experimental results showed that this broad spectral band processing technique offers an excellent coherent artifact noise suppression, and the technique is particularly suitable for color image deblurring. Experimental demonstrations and comparisons with the narrowband and coherent deblurring are also provided.

## I. Introduction

Restoration of smeared photographic images has long been an interesting and important application in optical processing.[1-7] In image deblurring much of the effort has been devoted to applying inverse filtering concepts to the image restoration. As those works evolved, two problems are still of intense interest; namely, the coherent artifact reduction and color image deblurring. Although Wiener filters had been applied in coherent processors by several investigations[1-6] for noise reduction, they do not suppress the inherent coherent artifact noise in the processing system. Recently, Yang and Leith[7] proposed a spatial domain deconvolution technique for image deblurring. They used an extended incoherent line source for deblurring, and the coherent noise was remarkably reduced. However, their technique is only suitable for processing monochrome blurred images. In previous papers[8-10] we presented a white-light processing technique for linearly smeared image deblurring. We have shown that the white-light image deblurring technique is capable of eliminating the coherent artifact noise and is suitable for color image deblurring. However, the results that we obtained were primarily restricted to the narrow spectral band deblurring concept.

In this paper we shall extend the image deblurring technique to the entire broad spectral band of the white-light source. To obtain the broadband deblurring effect, a fan-shaped spatial filter to compensate the scale of the Fourier spectra should be utilized at the Fourier plane. The technique of synthesizing the fan-shaped broadband deblurring filter is given. The coherence requirements for the white-light image deblurring are illustrated. Experimental demonstrations with the comparison of narrowband deblurring and coherent technique are provided.

## II. Broadband Image Deblurring

We shall now discuss a broadband image deblurring technique utilizing the entire spectral band of a white-light source. Let this linear smeared image be given, i.e.,

$$\hat{s}(x,y) = s(x,y) * \mathrm{rect}\left(\frac{y}{W}\right), \tag{1}$$

where $\hat{s}(x,y)$ and $s(x,y)$ are the smeared and unsmeared images,

$$\mathrm{rect}\left(\frac{y}{W}\right) \triangleq \begin{cases} 1, & |y| \le \dfrac{W}{2}, \\ 0, & \text{otherwise}, \end{cases} \tag{2}$$

and $W$ is the smeared length.

Let us insert the smeared image transparency of Eq. (1) into the input plane $P_1$ of a white-light optical processor as shown in Fig. 1. The complex light distribution for every wavelength $\lambda$ at the back focal length of the transform lens would be

$$E(\alpha,\beta;\lambda) = C' \iint \hat{s}(x,y,\lambda) \exp(ip_0 x) \times \exp\left[-i\frac{2\pi}{\lambda f}(x\alpha + y\beta)\right] dx\,dy, \tag{3}$$

where $p_0$ is the angular spatial frequency of the phase grating, $\alpha = [(\lambda f)/2\pi]p$ and $\beta = [(\lambda f)/2\pi]q$ represent the

The authors are with Pennsylvania State University, Electrical Engineering Department, University Park, Pennsylvania 16802.
Received 13 October 1982.
0003-6935/83/101439-06$01.00/0.

spatial coordinate system of Fourier plane $P_2$, $(p,q)$ is the corresponding angular spatial frequency coordinate system, $f$ is the focal length of the achromatic transform lens, and $C$ is an appropriate complex constant. Thus, Eq. (3) can be written as

$$E(\alpha,\beta;\lambda) = CS\left(\alpha - \frac{\lambda f}{2\pi} p_0, \beta\right), \tag{4}$$

where

$$S[\alpha - (\lambda f/2\pi)p_0,\beta] = S\left[\alpha - \left(\frac{\lambda f}{2\pi}\right)p_0,\beta\right] \operatorname{sinc}\left(\frac{\pi W}{\lambda f}\beta\right) \tag{5}$$

is the linear smeared image spectrum.

Since scale of the signal spectrum is proportional to the wavelength of the light source, the corresponding signal spectra would smear into a fan-shaped rainbow color as can be seen from Eq. (5). In other words, the top (i.e., the wider region) of the smeared spectra is in red and the bottom is in violet.

Let us assume that a fan-shaped broad spectral band deblurring filter (i.e., a broadband inverse filter) to accommodate the variation of the scale of the signal spectra is available. This fan-shaped filter is described in the following equation:

$$H(\alpha,\beta;\lambda) = \delta\left(\alpha - \frac{\lambda f}{2\pi} p_0,\beta\right)\left\{\int\left[\operatorname{rect}\left(\frac{y}{W}\right)\exp\left(-i\frac{2\pi}{\lambda f}\beta y\right)\right]dy\right\}^{-1},$$
$$= \delta\left(\alpha - \frac{\lambda f}{2\pi} p_0,\beta\right)\left[\operatorname{sinc}\left(\frac{\pi W}{\lambda f}\beta\right)\right]^{-1}. \tag{6}$$

In image deblurring we would insert this deblurring filter of Eq. (5) in the spatial frequency plane of $P_2$. The complex light distribution for every $\lambda$ at the output image plane $P_3$ can be written as

$$g(x,y;\lambda) = F^{-1}\left[S\left(\alpha - \frac{\lambda f}{2\pi} p_0,\beta\right) H(\alpha,\beta;\lambda)\right], \tag{7}$$

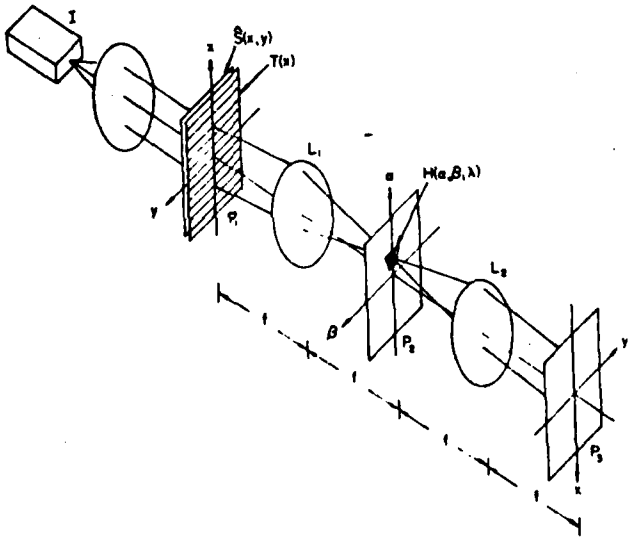


Fig. 1. White-light processor for smeared color image deblurring: $I$, white-light point source; $\hat{S}(x,y)$, smeared color image transparency; $T(x)$, diffraction grating; $L_1$ and $L_2$, achromatic transform lenses; $H(\alpha,\beta;\lambda)$, broad spectral band deblurring filter.

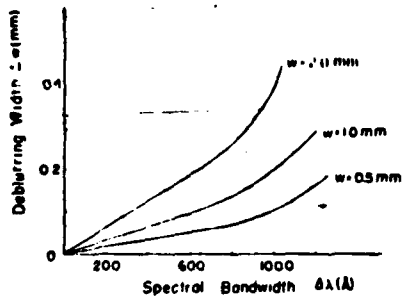


Fig. 2. Plots of the deblurring width $\Delta W$ as a function of the spectral bandwidth of the light source $\Delta\lambda$ for various values of smeared length $W$.

where $F^{-1}$ denotes the inverse Fourier transform; by substituting Eqs. (5) and (6) into Eq. (7), we have

$$g(x,y;\lambda) = s(x,y)\exp(ip_0 x), \tag{8}$$

which is independent of the wavelength of the light source. The resultant output intensity distribution can be shown as

$$I(x,y) = \int_{\Delta\lambda} |g(x,y;\lambda)|^2 d\lambda \simeq \Delta\lambda |s(x,y)|^2, \tag{9}$$

which is proportional to the entire spectral bandwidth $\Delta\lambda$ of the white-light source. Thus we see that this proposed white-light deblurring technique is capable of processing the information with the entire visible spectral band, and it is very suitable for the application to color-image deblurring. Since the integration of Eq. (9) is taken from the entire spectral band of the white-light source, the coherent artifact noise in principle can be eliminated.

## III. Coherence Requirement

Although this proposed deblurring technique utilizes a white-light source, the processing is operated in a partially coherent mode. It is, therefore, our aim in this section to discuss the basic coherence requirement for this proposed color image deblurring technique.

In a previous paper[11] we obtained the coherence requirements for a partially coherent optical processor. Several of those fruitful results can be applied to our proposed white-light image deblurring system.

We shall first discuss the temporal coherence requirement for the image deblurring. We shall use the results obtained in our previous article as shown in Fig. 2. This figure shows the plots of the spectral width $\Delta\lambda$ requirement of the light source (i.e., equivalent to the narrow spectral width of the deblurring filter) as a function of deblurred length ($\Delta W$) for various values of smeared length $W$. The wavelength spread across a narrow spectral band filter centered at wavelength $\lambda_0$[8,9] is

$$\Delta\lambda = \lambda_0|4\Delta p/p_0|, \quad p_0 \gg \Delta p, \tag{10}$$

or

$$\frac{\Delta p}{p_0} = \frac{\Delta\lambda}{4\lambda_0}, \tag{11}$$

where $\Delta p$ is the angular spatial frequency limit of the

Table I. Temporal Coherence Requirement for $\lambda_0 = 5461$ Å

| $\Delta p/p_0$ | 0.012 | 0.018 | 0.029 | 0.034 | 0.045 |
|---|---|---|---|---|---|
| $\Delta\lambda$ (Å) | 270 | 400 | 640 | 750 | 990 |
| $\Delta W/W$ | 1/20 | 1/15 | 1/10 | 1/8 | 1/5 |

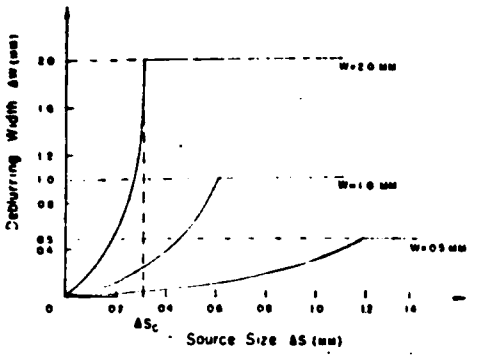


Fig. 3. Plots of the deblurring width as a function of the source size for various values of the smeared length $W$.

Table II. Effect of Spatial Coherence Requirement

| $W$ \ $\frac{\Delta W}{W}$, $\Delta s$ mm | 1/20 | 1/15 | 1/10 | 1/5 |
|---|---|---|---|---|
| 0.5 mm | 0.2 | 0.38 | 0.6 | 0.92 |
| 1 mm | 0.1 | 0.18 | 0.26 | 0.40 |
| 2 mm | 0.05 | 0.08 | 0.12 | 0.18 |

input blurred object transparency, and $p_0$ is the angular spatial frequency of the phase grating. The temporal coherence requirement for a narrow spectral band deblurring filter for wavelength 5461 Å is tabulated in Table I.

Although the temporal requirement is based on a narrow spectral band analysis, it can be extended to a broad spectral band operation. For example, a broad spectral band filter (e.g., fan-shaped deblurring filter) can be considered as a summation of a sequence of narrowband spatial filters of various wavelengths. The deblurred image is the result of the superposition of the mutually incoherent light fields derived from the narrowband filters. Thus, the temporal coherence requirement shown in Table I can also be applied to a broad spectral band filtering. As an example, if $(\Delta p)/p_0 = 0.012$ and the spectral bandwidth of the light source is 3000 Å, the broad spectral band deblurring filter is approximately equal to the sum of eleven narrow spectral band filters. The mean spectral bandwidth $\Delta\bar{\lambda}$ of those filters is 270 Å, and the deblurring ratio $(\Delta W)/W$ is 1/20. In other words, it is possible to synthesize a fan-shaped type spatial filter to compensate with the scale variation of the smeared Fourier spectra in the spatial frequency plane so that the deblurring takes place with the entire spectral band of the white-light source. Since the broadband deblurring utilizes the whole visible spectrum of the light source, it is particularly suitable for color image deblurring.

We shall now discuss the spatial coherence requirement. Since the deblurring operation acts on the smeared length, the coherence requirement is dependent on the width of the light source. Let us now use the plots of deblurring width as a function of the source size as shown in Fig. 3. From this figure we see that the deblurring effect (i.e., $\Delta W$) ceases when the source width $\Delta S$ reaches a critical width $\Delta S_c$. We shall now summarize the results of the spatial coherence requirement in Table II. From this table we see that the higher the degree of deblurring (i.e., smaller $\Delta W$), the more critical the spatial coherence (i.e., smaller the $\Delta S$) is required. It is, therefore, one of the prices we paid for a higher degree of deblurring.

## IV. Broadband Deblurring Filter Synthesis

We shall now briefly describe the synthesis of a fan-shaped (i.e., broad spectral band) deblurring filter. The synthesis is a combination of an absorptive-amplitude filter and a phase filter. A fan-shaped phase filter is composed of several slanted bar-type phase objects as illustrated in Fig. 4. Each phase bar would give rise to specific $\pi$ phase retardation for a predescribed dispersion of rainbow color wavelength. We note that the height of deblurring filter is, of course, dependent on the grating frequency $p_0$ at the input plane. The periodicity of the deblurred filter is certainly determined by the smeared length of the blurred object, and the width of the filter defines the degree of deblurring.[12] In constructing a broad spectral band phase deblurring filter, we utilize a vacuum deposition technique. It can be accomplished by depositing the magnesium fluoride ($MgF_2$) on this surface of an optical flat glass substrate. In this technique, a blocking mask of a fan-shaped bar pattern as shown in Fig. 4 is used for the vacuum deposition. The $MgF_2$ vapor is deposited through this blocking mask, together with a linear moving covering plate, from top to bottom as illustrated in Fig. 4.

The thickness of the deposited coating can be determined by the following equation:

$$d = \frac{\lambda}{2(n-1)}. \tag{12}$$

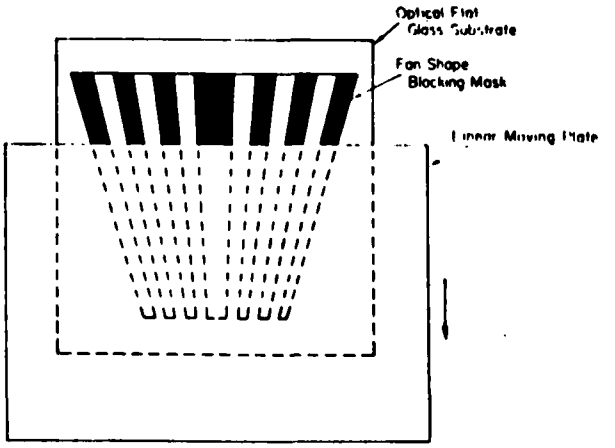


Fig. 4. Phase filter mask for $MgF_2$ vapor deposition.

where $n$ is the refractive index of the coating material. This coating thickness is linearly proportional to the dispersion of the illuminating wavelength. We note that a strictly linear control of coating thicknesses is very essential. The advantage of this phase type filter is to improve the transmission efficiency, since the overall deblurring filter is, in general, highly absorptive.

In principle, it is a straightforward method to synthesize a fan-shaped amplitude filter. The synthesis can be accomplished by inserting a slit aperture of a slit width equal to the smeared length of the blurred image at the input plane $P_1$ of the white-light optical processor shown in Fig. 1. The size of the white-light source should be adequately small under the spatial coherence regime to obtain a smeared sinc factor (i.e., smeared Fourier spectra of the slit aperture) in the Fourier plane. An amplitude filter can then be synthesized by simply recording this smeared sinc factor on a photographic plate. If the film-gamma of the recorded plate is controlled to about unity (i.e., $\gamma = 1$), the amplitude transmittance of the recorded plate is equivalent to that of the desired fan-shaped amplitude filter. However, in practice, a fan-shaped type amplitude filter is not that easy to synthesize due to three primary reasons. First, if a very small source size is required for the filter synthesis, it usually takes a longer exposure time, for example, if Kodak 649F plate (a low-speed film) is used. Second, the spectral response of the recording plate is generally not uniform for all visible wavelengths. The recorded filter would produce uneven transmittance in the direction of the smeared color spectra. The effect of the transmittance variation of the filter would affect the fidelity of color reproduction and the degree of restoration. Third, it is difficult to synthesize a sideband amplitude filter, since the dynamic range of the photographic film is very limited.

There is an alternative technique of generating a fan-shaped amplitude filter with coherent illumination as shown in Fig. 5. The purpose of using a curved-slit aperture is to accommodate the scale variation of the amplitude filter. The expression of the curved-slit aperture can be written

$$d(x,y;\lambda) = \operatorname{rect}\left(\frac{y}{W\lambda_0/\lambda}\right)\delta\left(x - \frac{\lambda f}{2\pi}p_0\right), \tag{13}$$

where $\lambda_0$ is the wavelength of the coherence source, $W$ is the smeared length of the blurred image, $f$ is the focal length of the cylindrical transform lens, and $\lambda$ is the wavelength of the white-light source.

The corresponding Fourier transformation of the curved-slit aperture can be shown as

$$D(\alpha,\beta;\lambda) = \operatorname{sinc}\left(\frac{\pi W}{\lambda f}\beta\right) * \delta\left(\alpha - \frac{\lambda f}{2\pi}p_0\right), \tag{14}$$

where * denotes the convolution operation.

It is clear now that a photographic recording of the spectra shown in Eq. (14) would produce a desirable fan-shaped amplitude filter for deblurring. In synthesis of this broadband amplitude filter, a He-Ne laser, with a rotating ground glass to reduce the artifact noise, is used as a coherent source. Kodak 131 plate is used for the recording plate, and a 6-min developing time in a POTA developer at 24°C is used to control the film gamma to about unity. The spectral wavelength limits are chosen from 4000 to 7000 Å. Within the dynamic range of the recording film, five sidelobes of ~300:1 dynamic range (or a density range of 2.5) are recorded with good accuracy. The fan-shaped amplitude filter obtained is tested with satisfactory results.

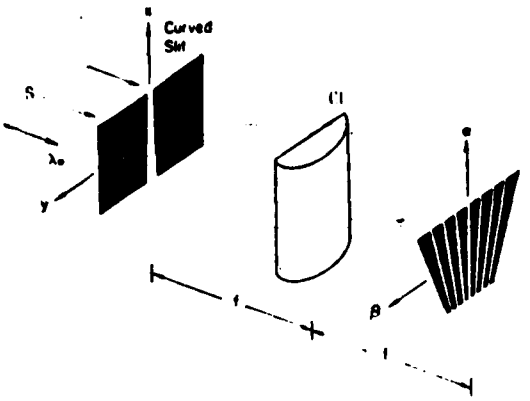


Fig. 5. Generation of amplitude filter. $S$ monochromatic plane wave; $CL$, cylindrical transform lens.

## V. Experimental Results

In this section we shall provide a few experimental results of image deblurring utilizing a broadband white-light source. In our experiments, a 75-W xenon arc lamp with a 200-$\mu$m pinhole is used as a broadband white-light source. A phase grating of 130 lines/mm with 25% diffraction efficiency at each first order diffraction is used at the input plane. An $f/8$ transform lens with 300-mm focal length is used for image Fourier transformation.

We shall first demonstrate the effect of the broadband deblurring as compared with the narrowband and the result obtained with coherent source. For simplicity of illustrations, we use a set of linear blurred alphabets as input objects as shown in Fig. 6(a). The smeared length is ~0.5 mm. Figure 6(b) shows the deblurred image obtained with this broadband deblurring technique, and the spectral bandwidth is ~3000 Å under white-light illumination. Figure 6(c) is the result obtained with a narrow spectral band deblurring filter of $\sim\Delta\lambda = 100$ Å centered at 6328 Å. Figure 6(d) is the deblurred image obtained with a He–Ne coherent source. In the comparison of these results, we see that the results obtained with a broad spectral band white-light source offers a higher deblurred image quality; for example, the coherent artifact noise is substantially suppressed, and the deblurred image appears to be sharper than the one obtained with a narrowband case.

We shall now experimentally demonstrate the capability of the white-light technique for color images. Figure 7(a) shows a black-and-white color blurred image of a building due to linear motion as an input color

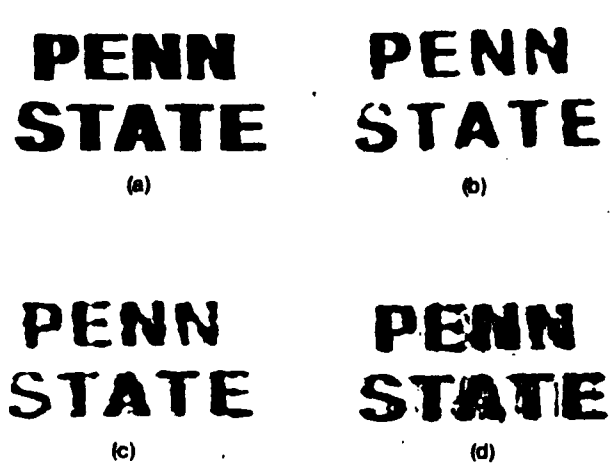


Fig. 6. Smeared image restoration of the words PENN STATE: (a) smeared image, (b) deblurred image obtained with broadband white-light source, (c) deblurred image obtained with narrow spectral band white-light source, and (d) deblurred image obtained with coherent source.

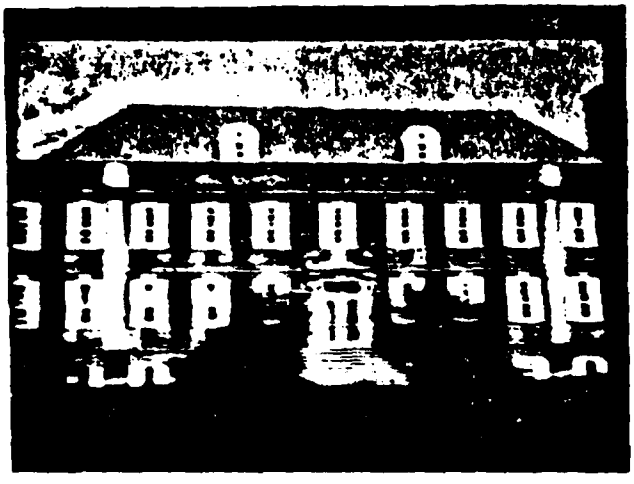

(a)

(b)

Fig. 7. Continuous-tone color image deblurring: (a) a black-and-white picture of a smeared color photograph of a building, (b) a black-and-white picture of the deblurred color image.

object. From this figure we see that the white window frames, the front doors, bushes, two white beams, trees, etc. are severely smeared. Figure 7(b) shows the deblurring result that we have obtained with this white-light processing technique. From this figure, we have seen that the color reproduction is rather faithful and the deblurred effect is spectacularly good; for example, the window frames, the bushes, the beams, the front doors, the trees, etc. can be clearly identified.

We would now provide another more striking example of the color image deblurring with this white-light processing technique. Figure 8(a) shows a black-and-white linear-motion blurred picture of an F-16 fighter plane. The body of this fighter plane is painted in blue-and-white colors, the wings are mostly painted red, the tail is blue-and-white, and the ground terrain is generally a bluish color. From this figure we see that the letters on the body on one of the wings and on this side of the tail are smeared beyond recognition. The details of the missiles at the tips of the wings are lost.

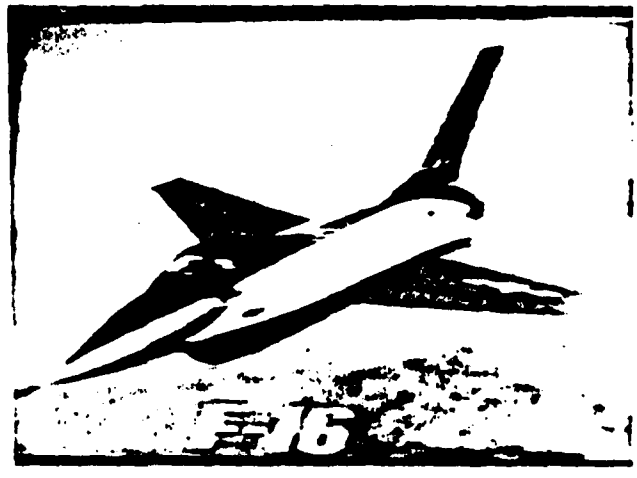

(a)

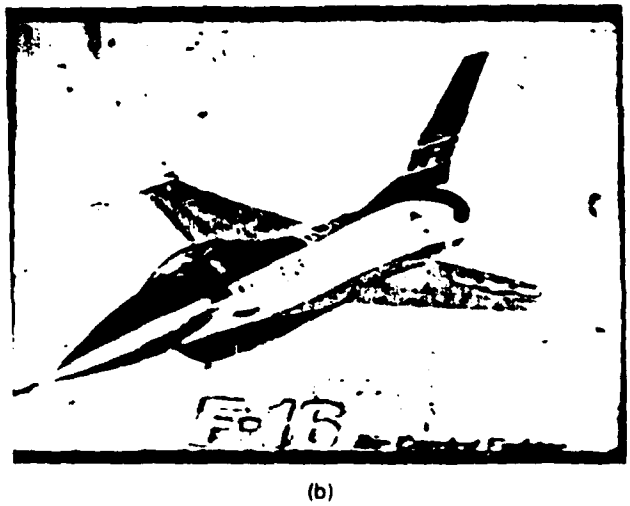

(b)

Fig. 8. Color image deblurring: (a) a black-and-white picture of a smeared color image of an F-16 fighter plane, (b) a black-and-white picture of the deblurred color image.

The star symbols at the tail end of the body and on the top of the wings are badly distorted. The features of ground terrain are obscured. Figure 8(b) shows the color image deblurring result that we have obtained from Fig. 8(a) with the proposed white-light deblurring technique. From this deblurred result, the letters USAF on the wing and YF-16 on the side of the tail can be clearly seen. The words U.S. AIR FORCE may be recognized. The star symbol on the wing can be clearly identified; however, the one on the body is rather obscured. Undoubtedly, the missiles at the tips of the wings can be seen, and the pilot in the cockpit is quite visible. The overall shape of the entire airplane is more distinctive than the blurred one. Moreover the river, the highways, and the forestry of the ground terrain are far more recognizable in this deblurred image. The color reproduction of the deblurred image is spectacularly faithful, and coherent artifact noise is virtually nonexistent. There is, however, some degree of color deviation inherently existing in the deblurred image. These are primarily due to chromatic aberration and the antireflectance coating of the transform lenses. Nevertheless, these two drawbacks can be overcome by utilizing good-quality achromatic transform lenses. A research program is currently underway to investigate this effect. Further improvement of the deblurring can also be accomplished by utilizing a blazed grating for high diffraction efficiency and a broader spatial bandwidth of the deblurred filter for a higher degree of deblurring. These two problems are also under current research.

## VI. Summary

We have shown a broadband color image deblurring technique utilizing a white-light source. This broad spatial band deblurring technique utilized a grating base method to obtain a dispersed smeared image spectra in the Fourier plane so that the deblurring operation can be taken placed in complex amplitude for the entire visible wavelengths. To perform this complex amplitude deblurring for the entire spectral band of the light source, we have shown that a fan-type deblurring filter to compensate the scale variation of the smeared signal spectra due to wavelength dispersion can be utilized. To alleviate the low transmission efficiency of the deblurring filter, we synthesized the deblurring filter with the combination of a broadband phase filter and a fan-shaped amplitude filter. The broad spectral band phase filter is synthesized by optical coating techniques, while the fan-shaped amplitude filter is obtained by a 1-D coherent processing technique.

By comparison of the results obtained by the broadband image deblurring with the narrow spectral band and coherent techniques, we have seen that the results obtained by the broadband deblurring offer a higher image quality. We have also shown that the broadband deblurring technique is very suitable for color image deblurring. We have provided several color image deblurring results obtained by the broadband deblurring technique. From these color deblurred images we have seen that the fidelity of the color reproduction is very high and the quality of deblurred image is rather good. Although there is some degree of color blur due to chromatic aberration of the transform lenses, it can be eliminated by utilizing higher-quality achromatic transform lenses.

Further improvements of the deblurring can also be obtained by utilizing a blazed grating to achieve a higher smeared spectral diffraction efficiency so that a wider spatial band deblurring filter can be used to achieve a higher degree of deblurring. Finally, we would like to point out that the utilization of higher-quality achromatic transform lenses and a blazed grating for the broadband image deblurring technique is currently under investigation.

We acknowledge the support of the U.S. Air Force Office of Scientific Research grant AFOSR-81-0148.

## References

1. J. Tsujiuchi, Prog. Opt. **2**, 133 (1963).
2. G. W. Stroke and R. G. Zech, Phys. Lett. A **25**, 89 (1967).
3. J. Tsujiuchi, T. Honda, and T. Fukaya, Opt. Commun. **1**, 379 (1970).
4. J. L. Horner, J. Opt. Soc. Am. **59**, 553 (1969).
5. J. L. Horner, Appl. Opt. **9**, 167 (1970).
6. R. M. Vasu and G. L. Rogers, Appl. Opt. **19**, 469 (1980).
7. G. G. Yang and E. N. Leith, Opt. Commun. **36**, 101 (1981).
8. F. T. S. Yu, Appl. Opt. **17**, 3571 (1978).
9. S. L. Zhuang, T. H. Chao, and F. T. S. Yu, Opt. Lett. **6**, 102 (1981).
10. F. T. S. Yu, S. L. Zhuang, and T. H. Chao, J. Opt. (Paris) **13**, 57 (1982).
11. S. L. Zhuang and F. T. S. Yu, Appl. Opt. **21**, 2587 (1982).
12. F. T. S. Yu, *Introduction to Diffraction, Information Processing, and Holography* (MIT Press, Cambridge, Mass., 1973), pp. 206–212.

# SECTION IV

## Pseudocolor Encoding with Three Primary Colors

Original article

*J. Optics (Paris)*, 1984, vol. *15*, n° 2, pp. 55-58

ELECTRICAL ENGINEERING DEPARTMENT
THE PENNSYLVANIA STATE UNIVERSITY
*University Park, PA 16802*

# WHITE-LIGHT DENSITY PSEUDOCOLOR ENCODING WITH THREE PRIMARY COLORS

F. T. S. YU, X. X. CHEN, T. H. CHAO

MOTS CLÉS :
Traitement des images
Pseudocouleurs

KEY WORDS :
Optical processing
Pseudocolors

SUMMARY : A technique of generating density pseudocolor encoding with three primary colors using a white-light optical processor is described. Spatial encodings are made with positive, negative, and product of positive and negative photographic-image transparencies, and the pseudocoloring is obtained by color filtering of the smeared Fourier spectra. The technique is simple, versatile, and economical to operate that may offer a wide range of applications. Since coherent sources are not utilized, the color coded image is free from coherent artifact noise. Experimental demonstrations of this density pseudocolor encoder are provided.

**Images codées par trois couleurs primaires**

RÉSUMÉ : On décrit une méthode de codage pseudocoloré avec trois couleurs primaires en utilisant un processeur optique en lumière blanche. Le codage pseudocoloré est fait en filtrant par des écrans colorés les spectres de transparents photographiques.

Le procédé est simple et il permet des applications variées dans de nombreux domaines. L'éclairage étant incohérent, on évite les défauts bien connus des images en lumière cohérente.

Quelques exemples montrent l'efficacité de la méthode

Most of the optical images obtained in various scientific applications and usually gray-level density images. For example, scanning electron microscopic images, multispectral band aerial photographic images, x-ray transparencies, etc. However, humans can perceive in color better than gray-level variations. In other words, a color coded image can provide a greater ability in visual discrimination.

In current practice, most of the pseudocolorings are performed by digital computer technique [1]. If the images are initially digitized, the computer technique may be a logical choice. However, for continuous tone images, optical color encoding technique [2] would be more advantageous for at least three major reasons : first, the technique in principle can preserve the spatial frequency resolution of the image to be color coded ; second, the optical system is generally easy and economical to operate ; third, the cost of an optical pseudocolor encoder is generally less expensive as compared with the digital counterpart.

Density pseudocolor encoding by halftone screen implementation with a coherent optical processor was first reported by Liu and Goodman [3], and later with a white-light processor by Tai, Yu and Chen [4]. Although good results have been subsequently reported, however there is a spatial resolution loss with the half-tone technique and number of discrete lines due to sampling are generally present in the color-coded image. A technique of density pseudocoloring through contrast reversal was recently reported by Santamaria *et al.* [5]. Although this technique offers the advantage over the halftone technique, the optical system is more elaborate and it requires both incoherent and coherence sources. Since the coherence source is utilized, the coherence artifact noise is unavoidable.

More recently a density pseudocolor encoding using a white-light processing technique was reported by Chao, Zhuang and Yu [6]. This technique offers the advantages of coherence noise reduction, no apparent resolution loss, versatility and simplicity of system operation, and low cost of pseudocoloring. Although excellent results have been reported by this technique, however pseudocolor encoding is primarily obtained by means two primary colors. We shall, in this paper, extend this white-light pseudocolor encoding technique for three primary colors. There is however one disadvantage of this proposed technique, it is still not a real-time pseudocolor encoding technique.

We shall now describe a simple white-light density

pseudocolor encoding technique for three primary colors. We assume that a x-ray transparency (called a positive image) is provided for pseudocoloring. By contact printing process, a negative x-ray image transparency is made. Let us now describe a spatial encoding technique to obtain a three-gray-level-image encoding transparency for the pseudocoloring. The spatial encoding is performed by respectively sampling the positive, negative, and the combination of both (i.e., the product of positive and negative) transparencies onto a black-and-white photographic film, with specific sampling grating frequencies oriented at specific azimuthal directions. To avoid the Moire fringe pattern, we shall sample these three images in orthogonal direction with different specific sampling frequencies, as proposed in *figure 1*. As an

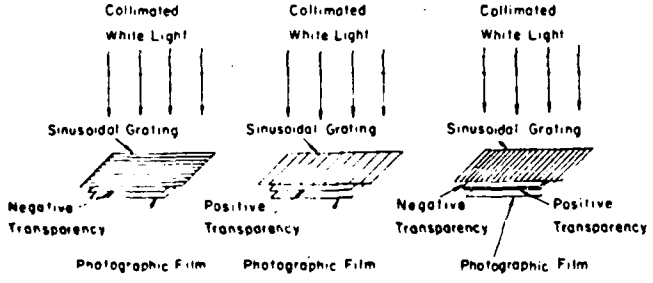


FIG. 1. — *Spatial encoding.*

illustration, the intensity transmittance of the encoded film can be written as

$$(1)\quad T(x, y) = K\{T_1(x, y)[1 + \operatorname{sgn}(\cos p_1 y)] + T_2(x, y)[1 + \operatorname{sgn}(\cos p_2 x)] + T_3(x, y)[1 + \operatorname{sgn}(\cos p_3 x)]\}^{-\gamma},$$

where $K$ is an appropriate proportionality constant, $T_1$, $T_2$, and $T_3$ are the positive, the negative, and the product image exposures, $p_1$, $p_2$, and $p_3$ are the respective carrier spatial frequencies, $(x, y)$ is the spatial frequency coordinate system of the encoded film, $\gamma$ is the film gamma, and

$$(2)\quad \operatorname{sgn}(\cos x) \triangleq \begin{cases} 1, & \cos x \geqslant 0, \\ -1, & \cos x < 0. \end{cases}$$

We shall now bleach the encoded transparency to obtain a surface relief phase object [7, 8]. We assume that the bleached transparency is encoded in the linear region of the diffraction efficiency $D$ *versus* log-exposure $E$ curve [8]. Thus, the amplitude transmittance of the bleached transparency can be written as

$$(3)\quad t(x, y) = \exp[i\phi(x, y)],$$

where $\phi(x, y)$ represents the phase delay distribution, which is proportional to the exposure of the encoded film [9], such as

$$(4)\quad \phi(x, y) = M\{T_1(x, y)[1 + \operatorname{sgn}(\cos p_1 y)] + T_2(x, y)[1 + \operatorname{sgn}(\cos p_2 x)] + T_3(x, y)[1 + \operatorname{sgn}(\cos p_3 x)]\},$$

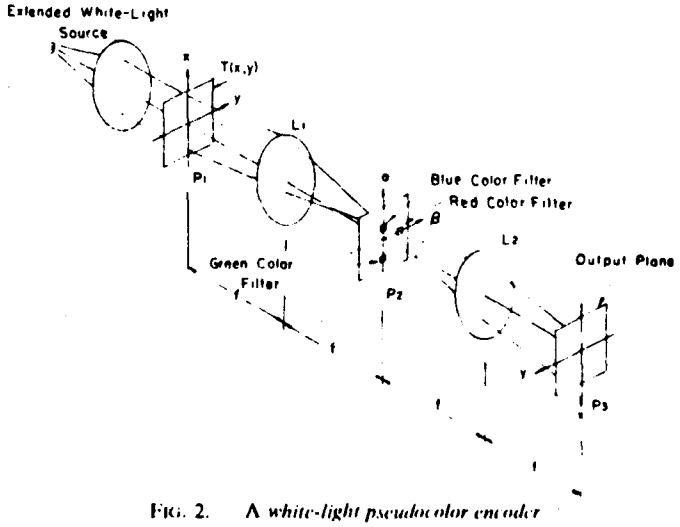


FIG. 2. — *A white-light pseudocolor encoder.*

where $M$ is an appropriate proportionality constant. If we place this bleached encoded film at the input plane $P_1$ of a white-light optical processor, as illustrated in *figure 2* then the complex light distribution due to $t(x, y)$, for every $\lambda$, at the spatial frequency plane $P_2$ can be determined by the following Fourier transformation :

$$(5)\quad S(\alpha, \beta; \lambda) = \iint t(x, y) \exp\left[-i\frac{2\pi}{\lambda f}(\alpha x + \beta y)\right] dx\, dy = \iint \exp[i\phi(x, y)] \exp\left[-i\frac{2\pi}{\lambda f}(\alpha x + \beta y)\right] dx\, dy.$$

By expanding $t(x, y)$ into an exponential series, Eq. (5) can be written as

$$(6)\quad S(\alpha, \beta; \lambda) = \iint \left\{1 + i\phi(x, y) + \frac{1}{2}[i\phi(x, y)]^2 + \cdots\right\} \exp\left[-i\frac{2\pi}{\lambda f}(\alpha x + \beta y)\right] dx\, dy.$$

By substituting Eq. (4) into Eq. (6) and retaining the first-order terms and the first-order convolution terms, we have :

$$(7)\quad S(\alpha,\beta;\lambda) = \hat{T}_1\left(\alpha,\beta \pm \frac{\lambda f}{2\pi}p_1\right) + \hat{T}_2\left(\alpha \pm \frac{\lambda f}{2\pi}p_2,\beta\right) + \hat{T}_3\left(\alpha \pm \frac{\lambda f}{2\pi}p_3,\beta\right) + \hat{T}_1\left(\alpha,\beta \pm \frac{\lambda f}{2\pi}p_1\right) * \hat{T}_2\left(\alpha \pm \frac{\lambda f}{2\pi}p_2,\beta\right) + \hat{T}_1\left(\alpha,\beta \pm \frac{\lambda f}{2\pi}p_1\right) * \hat{T}_3\left(\alpha \pm \frac{\lambda f}{2\pi}p_3,\beta\right) + \hat{T}_2\left(\alpha \pm \frac{\lambda f}{2\pi}p_2,\beta\right) * \hat{T}_3\left(\alpha \pm \frac{\lambda f}{2\pi}p_3,\beta\right),$$

where $\hat{T}_1$, $\hat{T}_2$ and $\hat{T}_3$ are the Fourier transforms of $T_1$, $T_2$ and $T_3$ respectively, * denotes the convolution operation, and the proportional constants have been neglected for simplicity. We note that, the last cross product term of Eq. (7) would introduce a Moire fringe pattern, which in the same sampling direction of $p_2$ and $p_3$. Nevertheless, all of these cross product terms can be properly masked out at the Fourier plane. Thus by proper color filtering the first-order smeared Fourier spectra, as shown in *figure 3*, a Moire free pseudocolor coded image can be obtained at the output plane $P_3$. The corresponding complex light field immediately behind the Fourier plane would be

$$(8)\quad S(\alpha,\beta) = \hat{T}_1\left(\alpha,\beta - \frac{\lambda_r f}{2\pi}p_1\right) + \hat{T}_2\left(\alpha - \frac{\lambda_b f}{2\pi}p_2,\beta\right) + \hat{T}_3\left(\alpha + \frac{\lambda_g f}{2\pi}p_3,\beta\right),$$

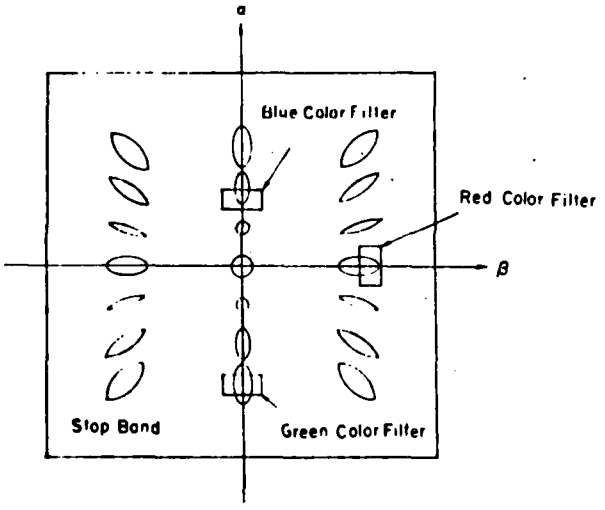


FIG. 3 — *Fourier plane color filtering.*

where $\lambda_r$, $\lambda_b$ and $\lambda_g$ are the respective red, blue, and green color wavelengths. At the output image plane, the pseudocolor coded image irradiance is therefore,

$$(9)\quad I(x,y) = T_{1r}^2(x,y) + T_{2b}^2(x,y) + T_{3g}^2(x,y),$$

which is a superposition of three primary color encoded images, where $T_{1r}$, $T_{2b}$, and $T_{3g}$ are the red, blue, and green amplitude distributions of the three spatially encoded images. Thus a Moire free color coded image can be obtained at the output plane.

In our experiment, we utilized two sinusoidal sampling gratings, one is 26.7 lines/mm and the other is 40 lines/mm for the spatial encodings. The encoding transparency was made by Kodak technical pan film 2415. The advantage of using Kodak 2415 film is that it is a low contrast film with a relatively flat spectral response. The plot of diffraction efficiency *versus* log-exposure for Kodak 2415 film at 40 lines/mm sampling frequency is shown in *figure 4*. From this figure, we see that the bleached encoded films offer a higher diffraction efficiency, the optimum value occurs at exposures $8.50 \times 10^{-3}$ mcs. With reference to this optimum exposure, it is possible to optimize the encoding process in the following : first, preexposuring the film beyond the shoulder region; second, subdividing the remaining exposure into three regions by taking the account of the transmittent exposures of the three encoded images.

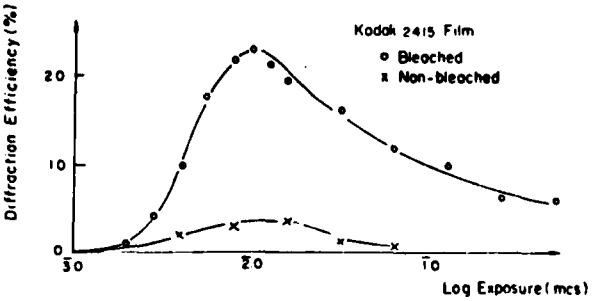


FIG. 4. — *Diffraction efficiency versus log exposure plot of a typical spatially encoded film.*

In pseudocoloring, we utilize the Kodak primary color filters of No. 25, 47B and 58 in the Fourier plane, as shown in *figure 3*. A xenon-arc lamp is used as extended white-light source for pseud lor encoded of *figure 2*.

For experimental demonstrations, we would first provide a gray-level x-ray picture of a front view female pelvis, as shown in *figure 5(a)*. *Figure 5(b)* shows the color encoded image obtained by the white-light pseudocolor encoder. In this color coded

(a).

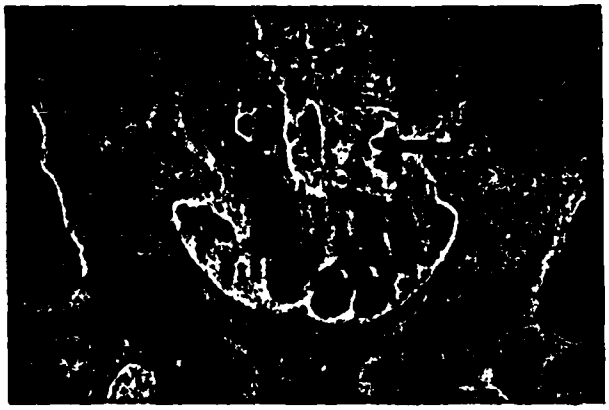

(b)

(c)

FIG. 5. — (a) *A gray-level x-ray picture* (b). *A density pseudocolor coded picture. Positive image is coded in red, negative image is coded in blue, and the product image is coded in green.* (c) *A reversal color coded image of figure 5* (b). *Positive image is coded in blue, negative image is coded in red, and the product image is again coded in green.*

image, the positive image is encoded in red, the negative image is encoded in blue, and the product transmittance of the positive and negative images is encoded in green. From this figure, we see that a broad range of pseudocolor encoded density can be perceived, and the color-coded image appears free from coherent artifact noise and Moire fringes. The patient of the x-ray picture appears to have suffered from a surgical operation, where the bore and point hardwares can be seen. A section of the bone, between the sacroiliac joint and spinal column, has been removed.

It may also be interesting to note that a reversal of the color encoding can be easily obtained by this white-light pseudocolor encoding technique, as shown in *figure 5(c)*. In this figure, the positive image is encoded in blue, the negative image is encoded in red, and the product transmittance is encoded in green. From this figure, again we see that a broad range density pseudocolor encoded image with different color textures can be obtained. For example the air pockets in the colon of the patient in *figure 5(c)* is much easier to be identified. In concluding this paper, we note that a wide variety of pseudocolor encoded images can easily be obtained by simply alternating the color filters in the Fourier plane of the white-light processor. The proposed white-light pseudocolor encoder is economical and easy to operate, which may offer many practical applications. There is, however, one disadvantage of this technique, it requires a spatial encoding process. Therefore, it is not a real-time pseudocolor encoding method.

We acknowledge the support of the U.S. Air Force Office of Scientific Research Grant AFOSR-81-0148.

## *REFERENCES*

[1] ANDREWS (H. C.), TESCHER (A. B.) and KRUGER (R. P.). — *IEEE Spectrum*, 9, 20 (1972).

[2] YU (F. T. S.). – Optical Information Processing. Wiley-Interscience Publishing Co., New York, 1982.

[3] LIU (H. K.) and GOODMAN (J. W.). — *Nouv. Rev. Opt.*, 7, 285 (1976).

[4] TAI (A.), YU (F. T. S.) and CHEN (H.) *Opt. Lett.*, 3, 190 (1978).

[5] SANTAMARIA (J.), GEA (M.) and BESCOS (J.) *J. Opt.*, 10, 15 (1979).

[6] CHAO (T. H.), ZHUANG (S. L.) and YU (F. T. S.), *Opt. Lett.*, 5, 230 (1980).

[7] UPATNIEKS (J.) and LEONARD (C.), *Appl. Opt.*, 8, 85 (1969).

[8] CHANG (B. J.) and WINICK (K.), *SPIE*, 215, 172 (1980).

[9] SMITH (H. M.). – « Basic Holographic Principles ». Ed. : H. M. Smith. Holographic Recording Materials. Springer-Verlag, New York, 1977.

*(Manuscript received in October 10, 1983.)*

# SECTION V

## Partial Coherence Measurement

Reprinted from Applied Optics, Vol. 23, page 333, January 15, 1984


# Coherence measurement of a grating-based white-light optical signal processor

F. T. S. Yu, F. K. Hsu, and T. H. Chao

A two-beam interference technique for coherence measurement in the Fourier plane of a grating-based white-light optical signal processor is presented. The visibility measurement is obtained with a scanning photometer at the output plane of the processor. The degree of coherence as a function of slit separation, due to source size, input object size, and the spatial frequency of the sampling grating, is plotted. The results show that the degree of coherence increases as the spatial frequency of the sampling grating increases. However, this improvement of coherence is somewhat more effective in the direction perpendicular to the light dispersion. Thus, this white-light signal processing technique is more effective in one dimension. Since this white-light processor is capable of processing the signal with the entire spectral band of the light source, it is very suitable for color image processing.

## I. Introduction

In the 1930s, work by Van Cittert[1] and later by Zernike[2] drew attention to the study of partial coherence. They have shown that the spatial coherence and the intensity distribution of the light source form a Fourier transform relationship. More recently, the work of Thompson[3-5] has demonstrated a two-beam interference technique to measure the degree of partial coherence. He has shown that, under quasi-monochromatic illumination, the degree of spatial coherence is dependent on the source size and the distance between two arbitrary points. The degree of temporal coherence is however dependent on the spectral bandwidth of the light source. He has also illustrated several coherence measurements that are consistent with the Van Cittert mode in the Fourier predictions.

We recently proposed a grating-based white-light optical signal processor.[6-8] We have shown that the white-light processor is capable of processing the information in complex amplitude like a coherent processor, and at the same time it suppresses the coherent artifact noise like an incoherent processor. In other words, this white-light processor is operating in a partially coherent mode in the Fourier plane as a partially coherent processor instead of an incoherent processor.

In this paper we shall describe a dual-beam technique for coherence measurement in the Fourier plane. We shall show that a high degree of coherence can be obtained in the spatial frequency plane such that the signal can be processed in complex amplitude for the entire spectral band of the white-light source.

## II. White-Light Optical Processing Technique

With reference to the schematic diagram of Fig. 1, the white-light optical processor is similar to that of a coherent optical processing system, except for the use of an extended white-light source, source encoding mask, signal sampling grating, and achromatic transform lenses. By the Wolf partial coherence theory,[9] the output intensity distribution can be obtained by the following integrating equations[10]:

$$I(x',y') = \int_{\lambda_l}^{\lambda_h} \iint_{-\infty}^{\infty} \gamma(x_0,y_0) \cdot \left| \iint_{-\infty}^{\infty} S\left(x_0 + \alpha - \frac{\lambda f}{2\pi} p_0, y_0 + \beta\right) H(\alpha,\beta) \times \exp\left[-i\frac{2\pi}{\lambda f}(x'\alpha + y'\beta)\right] \cdot d\alpha d\beta \right|^2 dx_0 dy_0 d\lambda, \quad (1)$$

where $\gamma(x_0,y_0)$ is the intensity distribution of the source encoder at the source plane $(x_0,y_0)$, $S(\alpha,\beta)$ is the Fourier spectrum of the input signal $s(x,y)$, $P_0$ is the angular spatial frequency of the grating, $f$ is the focal length of the achromatic transform lenses, $H(\alpha,\beta)$ is the complex spatial filter in the Fourier plane, $\lambda_l,\lambda_h$ are the lower

T. H. Chao is with University of Utah, Department of Electrical Engineering, Salt Lake City, Utah 84111; the other authors are with Pennsylvania State University, Electrical Engineering Department, University Park, Pennsylvania 16802.

Received 5 July 1983.
0003-6935/84/020333-08$02.00/0.

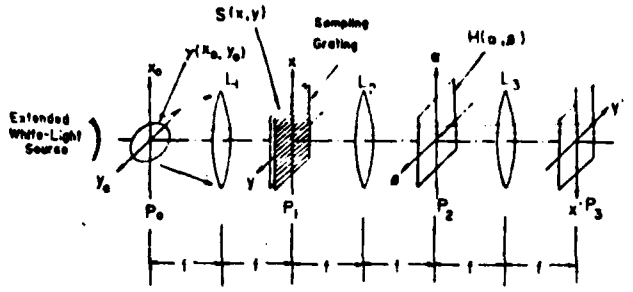


Fig. 1. Grating-based white-light optical signal processor: $\gamma(x_0,y_0)$, source encoding mask; $L$, achromatic transform lenses.

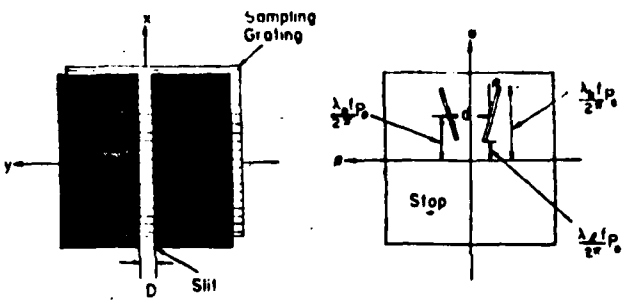


Fig. 2. Visibility measurement along the $\beta$ directions: $D$, input slit width; $d$, mean slit separation; $\lambda_0$, mean wavelength of the light source; $p_0$, angular spatial frequency of the sampling grating.

and upper wavelength limits of the light source, and $(\alpha,\beta)$ is the spatial coordinate system of the Fourier plane.

In optical signal processing, a set of $N$ narrow discrete spectral band filters $H_n(\alpha_n,\beta_n)$ over the rainbow color of Fourier spectra are used in the Fourier plane. Each of the spectral band filters is limited by a finite spectral bandwidth that can be approximated by the following equation[7,8]:

$$\Delta\lambda \simeq \frac{4\Delta p}{p_0}\lambda_n,\ p_0 \gg \Delta p. \tag{2}$$

where $\Delta p$ is the angular spatial frequency limit of the input signal in the $x$ direction, $p_0$ is the angular spatial frequency of the sampling grating, and $\lambda_n$ is the center wavelength of the filter $H_n(\alpha_n,\beta_n)$. Since the narrow spectral band filtered signals are mutually incoherent, the output intensity distribution of Eq. (1) can be written as

$$I(x',x') \simeq \sum_{n=1}^{N} I_n(x',y') \simeq \sum_{n=1}^{N} \int_{\lambda_0-\Delta\lambda_n/2}^{\lambda_0+\Delta\lambda_n/2} \iint_{-\infty}^{\infty} \gamma(x_0,y_0) \cdot \left| \iint_{-\infty}^{\infty} S\left(x_0+\alpha-\frac{\lambda f}{2\pi}p_0,y_0+\beta\right) H_n(\alpha_n,\beta_n) \times \exp\left[-i\frac{2\pi}{\lambda f}(x'\alpha+y'\beta)\right] d\alpha d\beta \right|^2 dx_0 dy_0 d\lambda. \tag{3}$$

With reference to Eq. (1) or (3), we see that the white-light signal processor is indeed capable of processing the signal in complex amplitude for the entire spectral band of the light source, and it is very suitable for color image processing. From these two equations, we also see that the degree of coherence is governed by the source encoding mask $\gamma(x_0,y_0)$, the spatial frequency of the sampling grating $p_0$, and the spatial frequency limit of the input signal $\Delta p$. In other words, the source encoding function is to improve the degree of spatial coherence at the input plane and the signal sampling grating is to increase the degree of temporal coherence in the Fourier plane, so that the signal processing can be carried out in complex amplitude at each narrow spectral band filter.

It is not hard to see from Fig. 1 that the signal spectrum is dispersed into rainbow color along the $\alpha$ axis in the Fourier plane. The improvement of the degree of coherence is expected to be more effective in the $\beta$ direction than in the $\alpha$ direction. In devising a coherence measurement scheme for this white-light optical processor, we propose a dual-beam interference technique for coherence measurement in the Fourier plane. For simplicity, we would however measure the degree of coherence in the $\beta$ and in the $\alpha$ axes independently.

## III. Coherence Measurement Technique

We shall now describe a visibility measurement technique to determine the degree of coherence in the $\beta$ direction in the Fourier plane. For simplicity, we shall utilize a narrow slit as a 1-D object at the input plane as shown in Fig. 2(a). The complex light distribution in the Fourier plane would be

$$E(\alpha,\beta;\lambda) = C\left[\operatorname{sinc}\left(\frac{\pi D}{\lambda f}\beta\right)\right] * \delta\left(\alpha-\frac{\lambda f}{2\pi}p_0,\beta\right). \tag{4}$$

where C represents an appropriate complex constant, $D$ is the slit width, $f$ is the focal length of the achromatic transform lens, $p_0$ is the angular spatial frequency of the phase sampling grating, and $*$ denotes the convolution operation.

It is clear that Eq. 4 describes a fan-shaped smeared Fourier spectrum of the input slit, for which the scale of the sinc factor increases as a function of the wavelength $\lambda$ of the light source and decreases as the size of the object $D$ (i.e., slit width) increases. To increase the efficiency of the coherence measurement along the $\beta$ direction, we would use a pair of slanted narrow slits at the smeared Fourier spectra, as illustrated in Fig. 2(b). The angle of inclination of this pair of slits should be adjusted with the separation of the slits, such as,

$$\theta = \tan^{-1}\frac{\pi d}{\lambda_0 f p_0}, \tag{5}$$

where $d$ is the mean separation of the slits, $\lambda_0$ is the mean wavelength of the light source, and $p_0$ is the angular spatial frequency of the sampling grating. The filtering function of this pair of slanted slits can be written as

$$H(\alpha,\beta) = \left[\delta\left(\beta-\frac{d\lambda}{2\lambda_0}\right)+\delta\left(\beta+\frac{d\lambda}{2\lambda_0}\right)\right] * \delta\left(\alpha-\frac{\lambda f}{2\pi}p_0,\beta\right). \tag{6}$$

The output intensity distribution can be shown as

$$I(x',y') = K[1+\cos(2\pi dx')], \tag{7}$$

where $K$ is an appropriate proportionality constant.

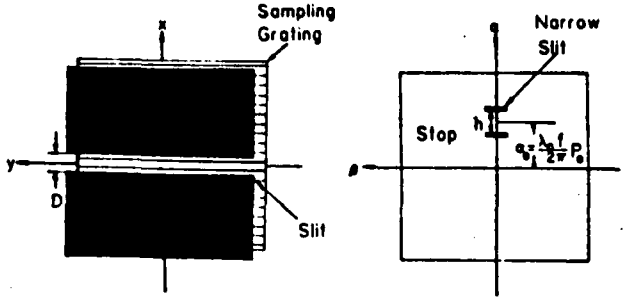


Fig. 3. Visibility measurement along the $\alpha$ direction: $D$, input slit width; $h$, slit separation; $\alpha_0$, center location of the pair of narrow slits; $\lambda_0$, mean wavelength of the light source; $p_0$, angular spatial frequency of the sampling grating.

Equation (7) represents an achromatic fringe pattern due to this entire spectral band of the light source.

Strictly speaking, all practical white-light sources are extended sources. For simplicity of illustration, we assume that an extended square source is used in this white-light optical processor. Thus the output intensity distribution can be written as

$$I(x',y') = \int_{\lambda_l}^{\lambda_h} \iint_{-\infty}^{\infty} \mathrm{rect}\left(\frac{x_0}{a}\right) \cdot \mathrm{rect}\left(\frac{y_0}{a}\right) \cdot \left| \iint_{-\infty}^{\infty} \mathrm{sinc}\left[\frac{\pi D}{\lambda f}(\beta + y_0)\right] * \delta\left(\alpha + x_0 - \frac{\lambda f}{2\pi} p_0, \beta\right) \cdot H(\alpha,\beta) \exp\left[-i\frac{2\pi}{\lambda f}(x'\alpha + y'\beta)\right] d\alpha d\beta \right|^2 dx_0 dy_0 d\lambda, \quad (8)$$

where $H(\alpha,\beta)$ is given by Eq. (6),

$$\mathrm{rect}\left(\frac{x_0}{a}\right) \triangleq \begin{cases} 1, & |x_0| \le a/2, \\ 0, & |x_0| > a/2, \end{cases}$$

and $a$ is the dimension of the extended light source. From the above equation we see that the visibility (i.e., degree of coherence) is dependent on the source size $a$, the object size $D$ (i.e., slit width), and the angular spatial frequency $p_0$ of the sampling grating.

To investigate the degree of coherence variation in the $\alpha$ direction, again we insert a narrow slit aperture as an input object but parallel to the sampling direction of the sampling grating, as shown in Fig. 3(a). The smeared Fourier spectra can be shown as

$$E(\alpha,\beta;\lambda) = \mathrm{sinc}\left(\frac{\pi D}{\lambda f}\alpha\right) * \delta\left(\alpha - \frac{\lambda f}{2\pi} p_0, \beta\right). \quad (9)$$

which describes a narrow smeared rainbow color spectra along the $\alpha$ axis. For the visibility measurement, a pair of narrow slits is inserted at the Fourier plane perpendicular to the $\alpha$ axis and centered at $\alpha = \lambda_0 f p_0/(2\pi)$, as shown in Fig. 3(b), where $\lambda_0$ is the center wavelength of the light source and $f$ is the focal length. The filtering function of this pair of slits can be written as

$$H(\alpha,\beta) = \delta\left(\alpha - \frac{h}{2} - \frac{\lambda_0 f}{2\pi} p_0, \beta\right) + \delta\left(\alpha + \frac{h}{2} - \frac{\lambda_0 f}{2\pi} p_0, \beta\right). \quad (10)$$

where $h$ is the separation between the slits. Again with the assumption of a square light source, the output intensity distribution can be shown as

$$I(x',y') = \int_{\lambda_l}^{\lambda_h} \iint_{-\infty}^{\infty} \mathrm{rect}\left(\frac{x_0}{a}\right) \mathrm{rect}\left(\frac{y_0}{a}\right) \cdot \left| \iint_{-\infty}^{\infty} \mathrm{sinc}\left[\frac{\pi D}{\lambda f}(\alpha + x_0)\right] * \delta\left(\alpha - \frac{\lambda f}{2\pi} p_0, \beta + y_0\right) \cdot H(\alpha,\beta) \exp\left[-i\frac{2\pi}{\lambda f}(x'\alpha + y'\beta)\right] d\alpha d\beta \right|^2 dx_0 dy_0 d\lambda, \quad (11)$$

where $H(\alpha,\beta)$ is defined in Eq. (10). From this equation, again we see that the degree of coherence in the $\alpha$ direction is dependent on the source size $a$, the object size $D$, and the angular spatial frequency $p_0$ of the sampling grating.

## IV. Experimental Results

The optical setup for the measurement of the degree of coherence in the Fourier plane of a grating-based white-light optical processor is shown in Fig. 4. This setup utilizes the principle of a dual-beam interference

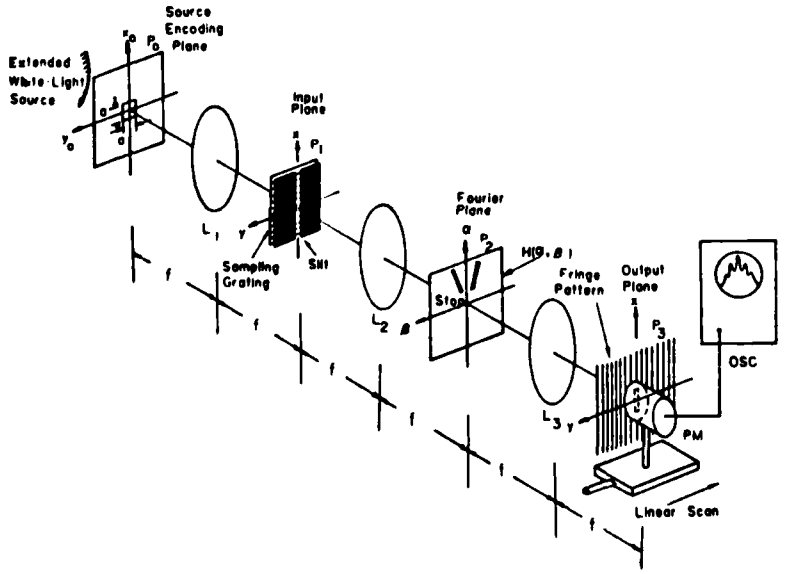


Fig. 4. Optical setup for the coherence measurement along the $\beta$ direction: $\gamma(x_0,y_0)$, source encoding mask; $a$, source size; $D$, input slit size; $L$, achromatic transform lenses; $H(\alpha,\beta)$ pair of slant slits; $PM$, photometer; $OSC$, oscilloscope.

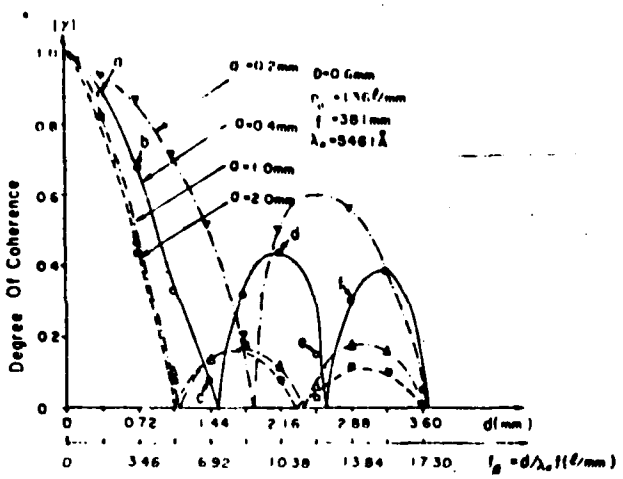


Fig. 5. Plots of degree of coherence along the $\beta$ direction as a function of mean slit separation $d$ for various values of source size $a$. $f_\beta = d/(\lambda_0 f)$, the mean slit separation in spatial frequency.

technique for coherence measurement. The output interference fringe pattern can be traced by a linear scanning photometer and displayed on an oscilloscope for the visibility measurement. In the experiment, the photometer is made by mounting a photomultiplier on the top of a motor-driven linear translator. Since it is a 1-D fringe pattern, a narrow slit can be utilized at the input end of the photomultiplier for the visibility measurement, i.e.,

$$V \triangleq \frac{I_{max} - I_{min}}{I_{max} + I_{min}}, \tag{12}$$

where $I_{max}$ and $I_{min}$ are the maximum and minimum intensities of the fringes. Needless to say that the visibility of the fringes is in fact a measure of the degree of coherence measurement,[8,9] i.e., $V = |\gamma|$, where $\gamma$ is the complex degree of coherence.

In the following we shall illustrate the visibility (i.e., coherence) measurement in the $\beta$ and $\alpha$ directions in the Fourier plane.

### A. Case I: Coherence Measurement in the $\beta$ Direction

We shall now describe the coherence measurement in the $\beta$ direction as illustrated in Fig. 4. We shall show that the visibility varies as functions of mean separation $d$ of the pair of slanted slits, source size $a$, object size $D$ (i.e., slit width), and spatial frequencies of the sampling grating. Figure 5 shows the variation of the degree of coherence as a function of main separation $d$ for various values of source sizes $a$. From this figure we see that the degree of coherence decreases as the separation $d$ increases. Further increase in $d$ increases the reappearance of the coherence. Still further increase in $d$ causes the repeated fluctuation of visibility. In this figure, we also see that the degree of coherence increases as the source size $a$ decreases. There is an interesting phenomenon in this coherence measurement. We see that as the source size $a$ decreases further, the reappearance of the visibility is higher. However the overall intensity of the smeared Fourier spectra decreases. This phenomenon is primarily due to the finite object size under a uniform source size illumination. Furthermore, if the source size $a$ is further increased, for example, exceeding 1.0 mm in Fig. 5, the decrease in coherence due to the source size is not apparent. This is primarily due to a comparable broader object size $D$ (e.g., $D$ = 0.6 mm) compared to a narrower sinc factor derived from source size $a$. Nevertheless, if the input slit size further decreases, the changes in degree of coherence for large source sizes can be seen.

We shall now provide a set of output fringe patterns with a set of normalized scanned photometer traces as shown in Fig. 6. The fringe patterns of Figs. 6(a) (c) were taken at visibilities of 0.88, 0.68, and 0.08 that correspond to the mean separations $d$ = 0.36, 0.72, and 1.44 mm at points $a$, $b$, and $c$ indicated on the main lobe of the plot $a$ = 0.4 mm in Fig. 5. Figures 6(d) and (e) were taken on the second lobe of the visibility reappearance that correspond to points $d$ and $e$ in Fig. 5. The degrees of coherence at these two points are 0.42 and 0.15, respectively. And the corresponding mean slit separations are 2.16 and 2.52 mm. Figure 6(f) was taken on the third lobe visibility at point $f$. The degree of coherence is 0.3 and the mean slit separation is 2.88 mm.

Let us now investigate the degree of coherence as a function of mean separation $d$ for various input object sizes $D$ (i.e., slit width) as plotted in Fig. 7. Again, we see that the degree of coherence decreases as $d$ increases. Further increase in $d$ also causes side lobes to reappear. In this figure we also see that the degree of coherence increases as object size $D$ decreases. Finally, Fig. 8 shows the visibility measure as a function of mean separation $d$ for two values of sampling grating frequencies. From this figure we see that the degree of coherence is dramatically improved in the Fourier plane by the insertion of the sampling grating.

### B. Case II: Coherence Measurement in the $\alpha$ Direction

At this stage we shall now measure the degree of coherence in the $\alpha$ direction in the Fourier plane. The measurement technique is essentially identical to that of Fig. 4, except the input object is replaced by a pair of horizontal slits as shown in Fig. 3. In coherence measurement, we centered the pair of slits at the center of the smeared Fourier spectra corresponding to $\lambda$ = 5461 Å.

Figure 9 shows plots of degree of coherence as a function of slit separation $h$ for various values of source sizes $a$. From this figure we see that the degree of coherence decreases as $h$ increases. Further increase in $h$ again causes the reappearance of the visibility side lobes. However, the degree of coherence is generally not affected by the variation of the source size $a$. Figure 10 shows a set of the visibility fringe patterns that we have obtained in the output image plane. This set of pictures was taken at points $a$, $b$, $c$, and $d$ as shown in Fig. 9. The corresponding degrees of coherence are

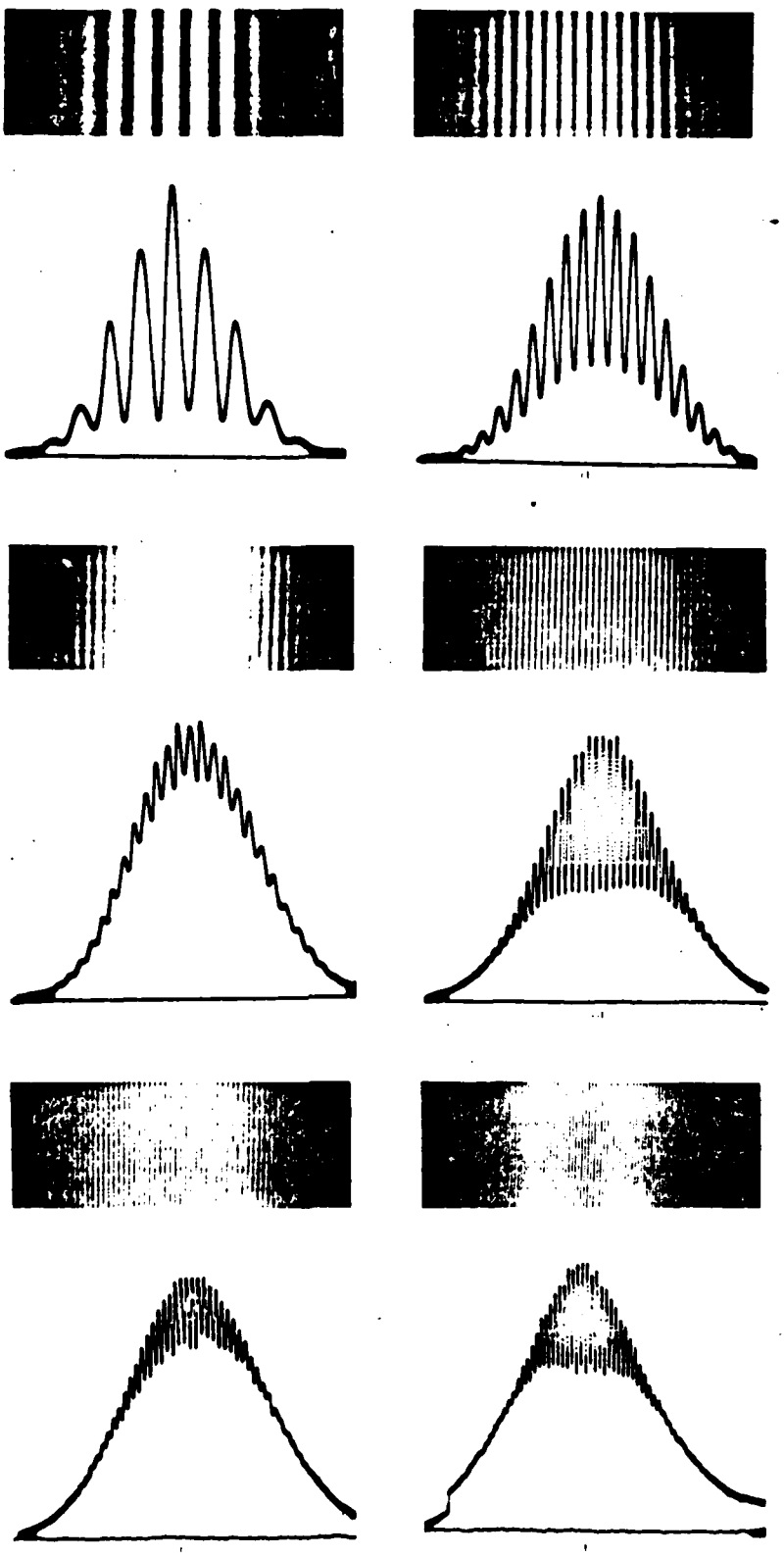

Fig. 6. Samples of fringe visibility patterns at the output plane. The upper portion of (a)–(f) shows the fringe visibility patterns. The lower portion shows the corresponding photometer traces. In these experiments, the fringe visibility and the spatial frequency were varied by changing the mean separation distance $d$ between the two slanted slits. (a)–(c) were obtained at points $a$, $b$, and $c$ on the first lobe of Fig. 5. These figures show the decrease in fringe visibility and corresponding increase in spatial frequency as the separation $d$ increases. (d) and (e) were obtained at points $d$ and $e$ on the second lobe of Fig. 5. These two figures also show the increase of spatial frequency as $d$ further increases. (f) was obtained at point $f$ on the third lobe of Fig. 5.

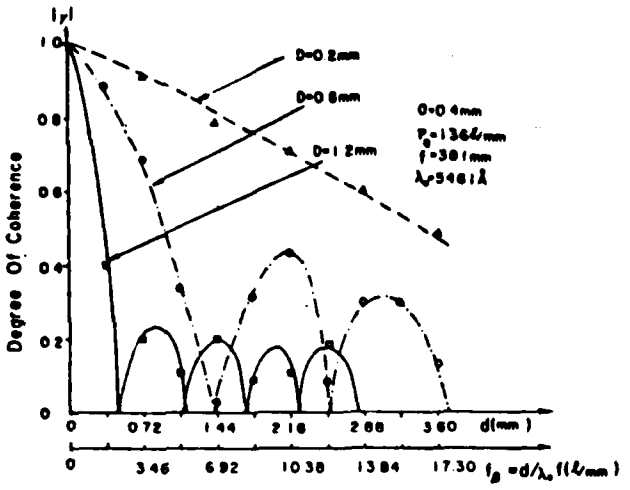


Fig. 7. Plots of degree of coherence along the $\beta$ direction as a function of mean slit separation $d$ for various values of input slit width $D$.

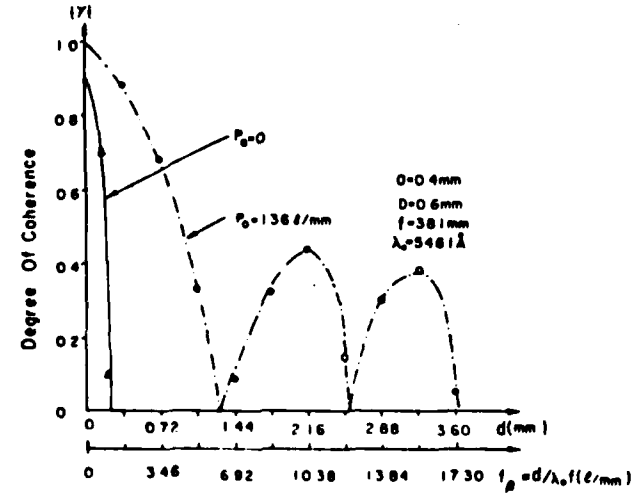


Fig. 8. Plots of degree of coherence along the $\beta$ direction as a function of mean slit separation $d$ for two values of sampling grating frequency $p_0$.

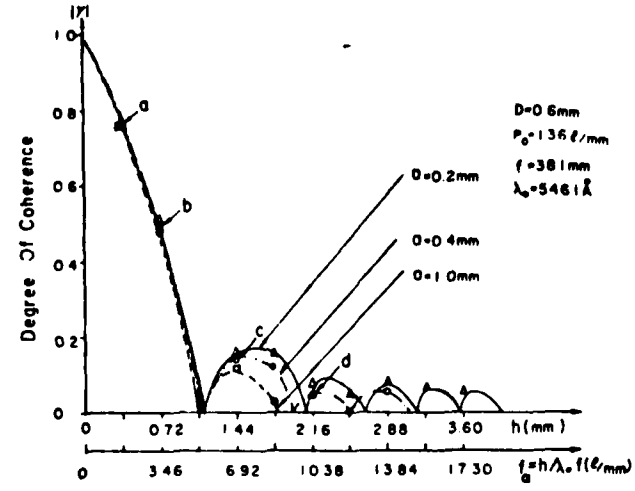


Fig. 9. Plots of degree of coherence along the $\alpha$ direction as a function of slit separation $h$ for various values of source size $a$. $f_\alpha = h/(\lambda_0 f)$, the corresponding slit separation in spatial frequency.

0.76, 0.50, 0.14, and 0.05. The respective separations are $h$ = 0.36, 0.72, 1.44, and 2.16 mm.

We shall now plot the degree of coherence as a function of $h$ for various values of object sizes $D$ (i.e., slit widths $D$) as shown in Fig. 11. From these plots we see that the degree of coherence decreases as the object size $D$ increases. Figure 12 shows the variation of coherence due to spatial frequency of the sampling grating as a function of slit separation $h$. From this figure we see that higher degree of coherence is achievable with the insertion of a high spatial frequency grating in the input plane.

We shall now briefly discuss the overall effect of coherence in the $(\alpha,\beta)$ spatial frequency plane. By comparing the visibility measurement of Figs. 5 and 9, we see that the degree of coherence substantially increases in the $\beta$ direction as the source size decreases. There is, however, no significant improvement in the $\alpha$ direction for smaller source sizes. Although both cases show the increase in coherence for smaller object sizes, however, the increase in coherence is higher in the $\beta$ direction compared with the $\alpha$ direction, as shown in Figs. 7 and 11. With reference to the plots of Figs. 8 and 12, both cases show significant improvement in the degree of coherence with the insertion of a sampling grating. However the improvement in coherence in the $\beta$ direction is somewhat higher than in the $\alpha$ direction, due primarily to overlapping of the smeared rainbow Fourier spectra.

To summarize these observations, we stress that the grating-based white-light optical signal processor does improve the degree of coherence in the Fourier plane. Although the higher degree of coherence is obtainable in both spatial frequency directions, the coherence improvement in the $\beta$ direction is generally higher. Thus, the white-light optical signal processing technique is generally more effective in the $\beta$ direction than in the $\alpha$ direction. We note that this effect can be seen in a recent paper on linear motion color image deblurring.[11]

## V. Conclusion

We have devised a dual-beam interference technique to measure the degree of coherence in the Fourier plane of a grating-based white-light optical signal processor. The effect of coherence variation due to source size, input object size, and the spatial frequency of the sampling grating is plotted as a function of distance in the $\beta$ and $\alpha$ directions of the Fourier plane. We have shown that the degree of coherence increases as the spatial frequency of the sampling grating increases. Although the improvement in degree of coherence in the Fourier plane is quite evident, the improvement in the $\beta$ direction (i.e., the direction perpendicular to the light dispersion) is somewhat more effective than in the $\alpha$ direction. The results indicate that this white-light optical signal processing technique is somewhat more effective in the $\beta$ direction than in the $\alpha$ direction. Nevertheless the existence of the high degree of coherence in the Fourier plane allows us to process the in-

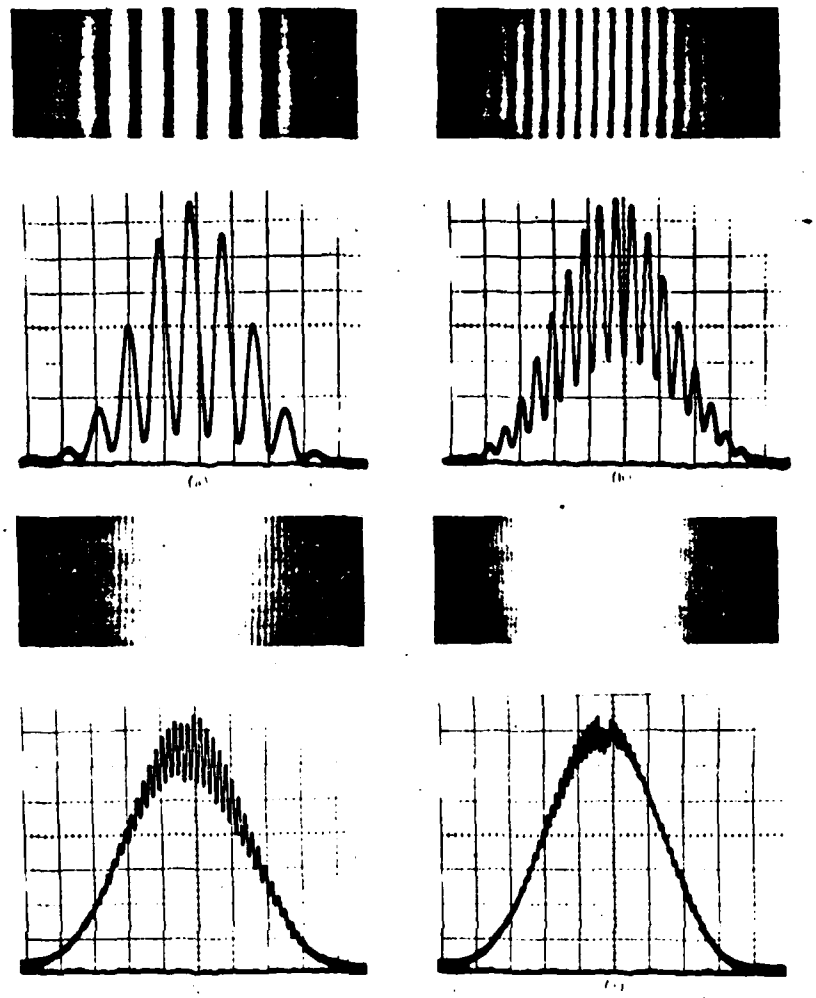

Fig. 10. Samples of fringe visibility patterns. The upper portion of (a)–(d) shows fringe visibility patterns; the lower portion shows the corresponding intensity profiles. (a) and (b) were obtained at points *a* and *b* on the first lobe of Fig. 9. (c) was obtained at point *c* on the second lobe of Fig. 9, and (d) was obtained at point *d* on the third lobe of Fig. 9.

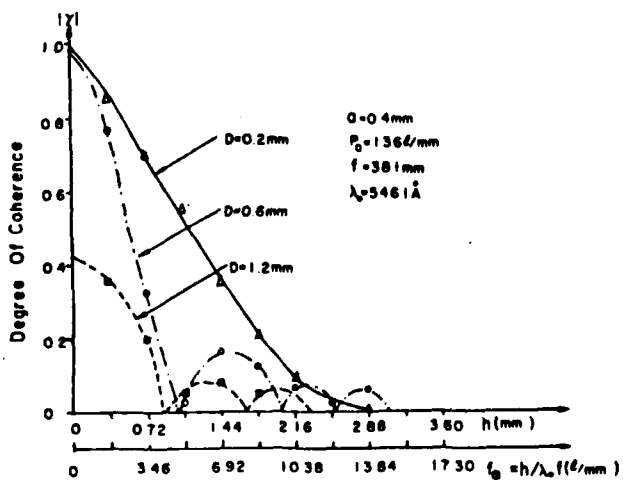


Fig. 11. Plots of degree of coherence along the $\alpha$ direction as a function of slit separation $h$ for various values of object size $D$.

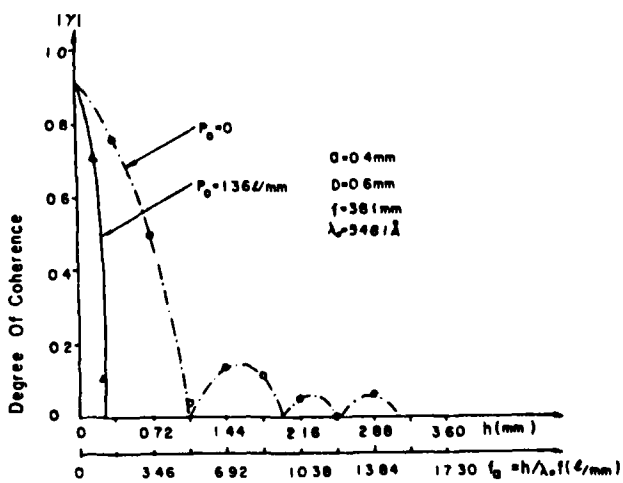


Fig. 12. Plots of degree of coherence along the $\alpha$ direction as a function of slit separation $h$ for two values of sampling grating frequency $p_0$.

formation in complex amplitude rather than in intensity. And the white-light processing technique is very suitable for color signal processing.

We acknowledge the support of the U.S. Air Force Office of Scientific Research grant AFOSR-81-0148.

## References

1. P. H. Van Cittert, Physica **1**, 201 (1934).
2. F. Zernike, Physica **5**, 785 (1938).
3. B. J. Thompson, J. Opt. Soc. Am. **48**, 95 (1958).
4. B. J. Thompson and E. Wolf, J. Opt. Soc. Am. **47**, 895 (1957).
5. B. J. Thompson, Proc. Soc. Photo-Opt. Instrum. Eng. **4**, 7 (1965).
6. F. T. S. Yu, Opt. Commun. **27**, 23 (1978).
7. F. T. S. Yu, Proc. Soc. Photo Opt. Instrum. Eng. **232**, 9 (1980).
8. F. T. S. Yu, *Optical Information Processing* (Wiley-Interscience, New York, 1983).
9. M. Born and E. Wolf, *Principles of Optics* (Pergamon, New York, 1980).
10. S. L. Zhuang, and F. T. S. Yu, Appl. Opt. **21**, 2587 (1982).
11. T. H. Chao, S. L. Zhuang, S. Z. Mao, and F. T. S. Yu, Appl. Opt. **22**, 1439 (1983).

# SECTION VI

## Restoration of Out-of-Focused Color Image

Volume 46, number 5,6 OPTICS COMMUNICATIONS 15 July 1983

# RESTORATION OF OUT-OF-FOCUSED COLOR PHOTOGRAPHIC IMAGES

X.J. LU and F.T.S. YU
*Electrical Engineering Department, The Pennsylvania State University, University Park, PA 16802, USA*

Received 14 March 1983

A method of deconvoluting the defocused color photographic images utilizing a white-light processing is described. In the white-light processing, a diffraction grating is used to provide three primary color light sources for the color image restoration. Three complex inverse filters, for each primary color, are used in the Fourier transform plane. Experimental demonstrations of the color image restoration of defocused photographic images are given.

## 1. Introduction

Restoration of blurred photographic images has long been an interesting application in optical signal processing [1–8]. We have in previous papers [9–12] presented a white-light processing technique for linearly smeared image deblurring. We have shown that the white-light image deblurring technique is capable of suppressing the coherent artifact noise and is suitable for color image deblurring. However the results that we had obtained were primarily restricted to blurred due to linear motion.

In this paper, we shall extend the white-light image restoration technique to two-dimensional image deblurring. We shall utilize a white-light source for the restoration of the out-of-focused color photograph images. The proposed color image restoration technique includes three primary color sensitive inverse filters, as shown in fig. 1. In this figure, a high diffraction efficient grating is used at plane $P_{01}$ to produce three orders of smeared color spectra at the back focal plane $P_{02}$. Three pinholes (one with a blue filter) are properly placed over this set of spectral lights, to produce three primary color point sources (i.e., spatially small) at plane $P_{02}$. In the Fourier transform plane $P_2$, three color sensitive inverse filters are used for the restoration, and the deblurred color images can be seen at the output plane of the optical processor.

## 2. Defocused color image restoration

With reference to the optical processor of fig. 1, there are three primary color point sources derived from a white-light source. The intensity distribution of these three primary color point sources can be represented by the following equation

$$I(\alpha,\beta;\lambda) = K_B \operatorname{cir}|(\alpha^2+\beta^2)^{1/2}/d_B| + K_R \operatorname{cir}|((\alpha+\lambda_R f p_0)^2+\beta^2)^{1/2}/d_R| + K_G \operatorname{cir}|((\alpha-\lambda_G f p_0)^2+\beta^2)^{1/2}/d_G| , \quad (1)$$

where $\operatorname{cir}|X| \doteq 1$, $|X| \leqslant 1$, and 0 otherwise; $(\alpha,\beta)$ is the spatial coordinate system of plane $P_{02}$, $p_0$ is the spatial frequency of the diffraction grating, $T(x)$, $f$ is the focal length of the achromatic transform lens, $K_B, K_R, K_G$ are the proportional constants, $d_B, d_R, d_G$ are diameters of the pinholes, and $\lambda_B, \lambda_R, \lambda_G$ are the center wavelengths of the blue, red, green spectral bands of the light sources, respectively. For red and green point sources, the center wavelength of each spectral band would be

$$\lambda = \alpha/f p_0 , \quad (2)$$

which is determined by the position of the pinhole at $\alpha$ axis. The corresponding spectral bandwidth $\Delta\lambda$ of the point sources can be written as



0 030-4018/83/0000–0000/$ 03.00 

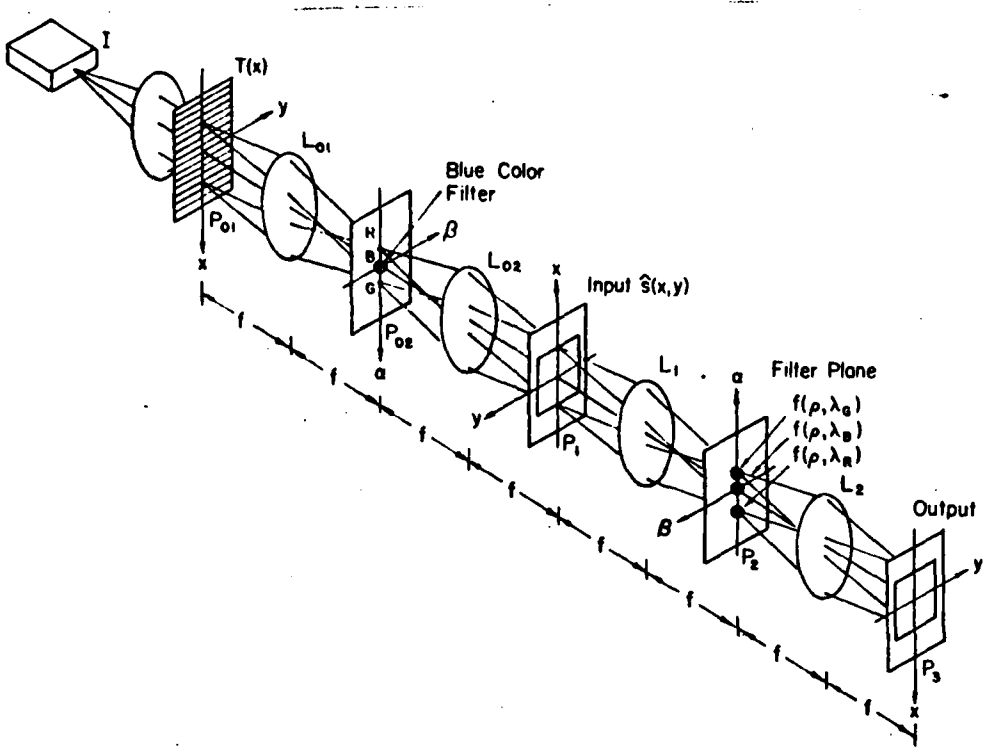


Fig. 1. A white-light optical processor for out-of-focused color image deblurring. I; white-light source, $T(x)$; diffraction grating, R, B, G; red, blue, and green color sources, $S(x,y)$; out-of-focused color image, L; achromatic transform lenses, $f(\rho, \lambda_G)$, $f(\rho, \lambda_B)$, $f(\rho, \lambda_R)$, inverse filters for green, blue, red light.

$$\Delta\lambda = \Delta\alpha/fp_0 = d/fp_0 , \tag{3}$$

where $d$ is the diameter of the pinholes.

We note that the complex degree of coherence produced by the color point sources at the input plane $P_1$ of the processor is [13]

$$\mu_n = \frac{2J_1(\pi d_n r_n)}{\pi d_n r_n} \exp(i2\pi\phi_n x), \quad n = R,G,B , \tag{4}$$

where $J_1$ is the first-order Bessel function, $r_n = (1/\lambda_n f)(x^2 + y^2)^{1/2}$, and $\phi_n = 0, -\lambda_R p_0$, and $\lambda_G p_0$ for the blue, red, and green color point sources, respectively. Since the transform lens $L_{02}$ is achromatic, the spatial coherence length produced by a circular point source would be

$$R = Kf\lambda/d , \tag{5}$$

where $K$ is a proportionality constant, and $K = 1.22$ if the spatial coherence length $R$ is defined as the distance in which the degree of coherence $\mu$ drops from unit to first zero value. If $R$ is defined from a drop of 12% from the unit degree of coherence, then $K = 0.32$. With reference to eqs. (3) and (5), we note that

$$R = K\lambda/\Delta\lambda p_0 . \tag{6}$$

Thus to maintain the same spatial coherence length and the same spectral bandwidth, different spatial frequency $p_0$ of the grating should be used. However, with the use of multi-grating frequency, it would reduce to available power of the light source for the processing. Nevertheless this problem can be alleviated by using a single diffraction grating at $P_{01}$ and different sizes of pinholes at $P_{02}$ plane. In this manner the same spatial coherence length can be obtained by simply varying the size of the pinholes of the primary color sources. As a numerical example; we tabulate the requirement of the size of the pinholes, spatial coherence lengths, and the spectral bandwidths of the

Table 1
Relationship of size, spectral bandwidth and spatial coherence length of three color sources.

| λ (Å) | $d$ (μm) | Δλ (Å) | $K$ | $R$ (mm) |
|---|---|---|---|---|
| 6300 red | 400 | 290 | 0.32 | 0.18 |
| | | | 1.22 | 0.67 |
| | 200 | 140 | 0.32 | 0.35 |
| | | | 1.22 | 1.35 |
| 5500 green | 400 | 290 | 0.32 | 0.15 |
| | | | 1.22 | 0.59 |
| | 170 | 120 | 0.32 | 0.36 |
| | | | 1.22 | 1.38 |
| 4300 blue | 400 | 500 | 0.32 | 0.12 |
| | | | 1.22 | 0.46 |
| | 140 | 500 | 0.32 | 0.34 |
| | | | 1.22 | 1.31 |

Note: Δλ = 500 Å for blue wavelength λ = 4300 Å is limited by Kodak 47B filter.

sources, in table 1. If the pinholes for red and green sources are of the same diameter, e.g., $d_R = d_G = 400$ μm, the spectral bandwidths would be Δλ = 290 Å. On the other hand, if the three pinhole diameters are different, e.g., $d_R = 200$ μm, $d_G = 170$ μm, and $d_B = 140$ μm, coherence lengths obtained would be similar, i.e., 1.35 mm (red), 1.38 mm (green), and 1.31 mm (blue).

In filter synthesis, we note that the inverse filter function for the restoration of out-of-focus image, for each primary color wavelength, should be

$$f(\rho,\lambda) = \begin{cases} \dfrac{\pi a\rho}{2J_1(\pi a\rho)}\,\dfrac{1}{m}\,, & |f(\rho,\lambda)| \leqslant 1\,, \\ \pm 1\,, & \text{otherwise}\,, \end{cases} \tag{7}$$

where $a$ is the diameter of the defocused point spread function, $\rho = (1/\lambda f)(\alpha^2+\beta^2)^{1/2}$, and $m$ is a constant of the order of 10 to $10^2$. The meaning of $m$ is that the finite filter in dynamic range can be made in physical sense because $J_1(\pi a\rho)$ has an infinite number of zeros [1]. Needless to say that eq. (7) can also be written as

$$f(\rho,\lambda) = |f(\rho,\lambda)|\,e^{i\theta}\,.$$

Thus an inverse filter can be synthesized by the combination of an amplitude and a phase filter. The amplitude filter can be synthesized by recording an amplitude spectrum of a circular aperture of a given diameter using a He-Ne laser. Since the scale of the spectrum is proportional to the wavelength, the diameter of the circular aperture should be properly fitted with the color wavelength. In other words, the diameter for the red amplitude filter should be smaller than the green amplitude filter, and the diameter for the green filter should be smaller than the blue. For example, if the diameter of the circular aperture for red light is taken equal to 0.5 mm, then the diameter of the aperture for the green should be 0.58 mm, and the diameter for the blue light should be 0.74 mm. In amplitude filter synthesis, it is necessary to control the gamma of the recording plate equal to 1 to obtain the required amplitude transmittance.

In phase filter synthesis, we see that, the filter is primarily composed of a set of π-phase circular concentric rings, as shown in fig. 2. The diameters of the rings are determined by the primary color wavelength and the size of the defocused point spread function. A simple technique of producing the phase filter is a bleaching method [14]. A black-and-white ring pattern, corresponding to the π-phase zone of the phase filter, is recorded on a high-contrast film. The recorded binary ring pattern is used as a mask to reproduce a number of gray-level rings on a low-contrast photographic plate. If the recorded plate is bleached, a set of deblurring phase filters can be obtained. To search for a π-phase filter for a given wavelength, one can

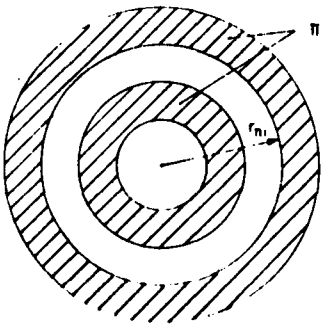


$$r_{ni} = \frac{x_i \lambda_n f}{a}\,,$$

where $J_1(\pi x_i) = 0$, $i = 1,2,3,4$,
$\lambda_n = \lambda_R(6300\text{Å}),\ \lambda_G(5500\text{Å}),$
$\lambda_B(4300\text{Å})$,
$a = 0.5\,\text{mm}$, $f = 350\,\text{mm}$.

Fig. 2. A π-phase concentric rings for a deblurring phase filter.

utilize the contrast-reverse method or by observing the intensity ratio of the main peak and the second peak of a processed point spread function.

In this manner, a set of deblurring filters suitable for the three primary color wavelengths can be obtained. The primary color inverse filter functions can be described as

$$f(\rho_n, \lambda) = \frac{\pi a \rho_n}{2J_1(\pi a \rho_n)} \frac{1}{m} , \quad n = \mathrm{R,G,B} , \tag{8}$$

where

$$\rho_n \triangleq (1/\lambda_R f)((\alpha + \lambda_R f p_0)^2 + \beta^2)^{1/2} , \quad \text{for } \lambda_R ,$$

$$(1/\lambda_G f)((\alpha - \lambda_G f p_0)^2 + \beta^2)^{1/2} , \quad \text{for } \lambda_G ,$$

$$(1/\lambda_B f)(\alpha^2 + \beta^2)^{1/2} , \quad \text{for } \lambda_B .$$

The three inverse filters are placed in the Fourier plane $P_2$ of the processor, their positions should be adjusted properly, such that $\alpha = -\lambda_R f p_0, \beta = 0$ for red sensitive inverse filter, $\alpha = \lambda_G f p_0, \beta = 0$ for green, and $\alpha = 0$, $\beta = 0$ for blue.

## 3. Experimental results

In our experiment, a 75 W xenon arc lamp with a 500 $\mu$m pinhole is used as the white-light source I. A phase grating of 40 ℓ/mm is placed at plane $P_{01}$, and three pinholes of 200 $\mu$m, 170 $\mu$m, and 150 $\mu$m, for the red, green, and blue spectral bands are used at plane $P_{02}$. The center wavelength for the red spectral band is 6300 Å, 5500 Å for the green, and 4300 Å for the blue. Since we utilize the zero-order spectra for the blue color source, a Kodak 47B blue color filter is used to cover the pinhole. The spectral bandwidths of these primary color sources are: 140 Å for the red, 120 Å for the green, and 500 Å for the blue. Needless to say that the intensities of these three primary color sources can be adjusted by a set of neutral density filters for color balance.

For the first experimental demonstration, we used a circular aperture of about 0.5 mm in diameter as a defocussed point spread function, as shown in fig. 3a. Fig. 3b shows the restored image of fig. 3a obtained with this polychromatic restoration technique. From this figure, we see that, the deblurred point spread function mainly consists of a high intensity center peak, as the deblurred image, and a weak circular ring image, which is primarily due to the finite extent of the deblurring filters. In our experiment the deblurring filters are limited to about four lopes, and the greatest density of the amplitude filter is about 2 to 2.5 D.

From the result of fig. 3b, we also see that there is a slight color dispersion at two edges of the center restored peak image. We note that, the dispersion is

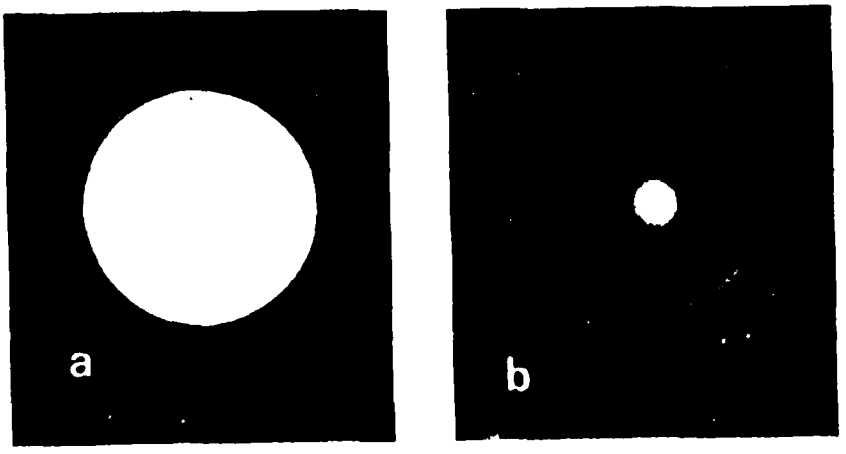


Fig. 3. Restoration of a defocused point spread function. a) A transparent circular disk as a defocused point spread function. b) A black-and-white picture of the deblurred point spread-function.

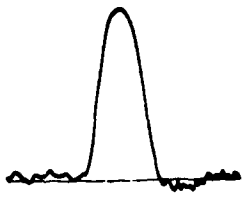

Fig. 4. A electronic scanned image of fig. 3b.

primarily due to the chromatic aberration of the transform lenses, which can be eliminated by using higher quality achromatic transform lenses. Fig. 4 shows an electronic scanned image of the result of fig. 3b. From this figure, we see that the intensity of the center peak is much higher than that of the first-order ring.

We now provide a second experimental demonstration for three overlapping primary color disks, as shown in fig. 5a. The size of these primary color disks are about 0.5 mm in diameter. If the color transparency of fig. 5a is inserted at the input plane of the proposed deblurring processor of fig. 1, the restored color point images can be obtained, as shown in fig. 5b. From this figure we see that the color of the restored images are very faithful. However there is a slight replacement of the deblurred color point image, which is primarily due to the chromatic aberration of the transform lenses.

As a final experimental result, fig. 6a shows two blurred color words (i.e., "Color Image") as an input blurred image. The corresponding deblurred color image obtained with this deblurring technique is shown in fig. 6b. From this deblurred color image, again we see that the color reproduction is rather faithful and the quality of the deblurred image is quite impressive. Since the color image deblurring is obtained with three

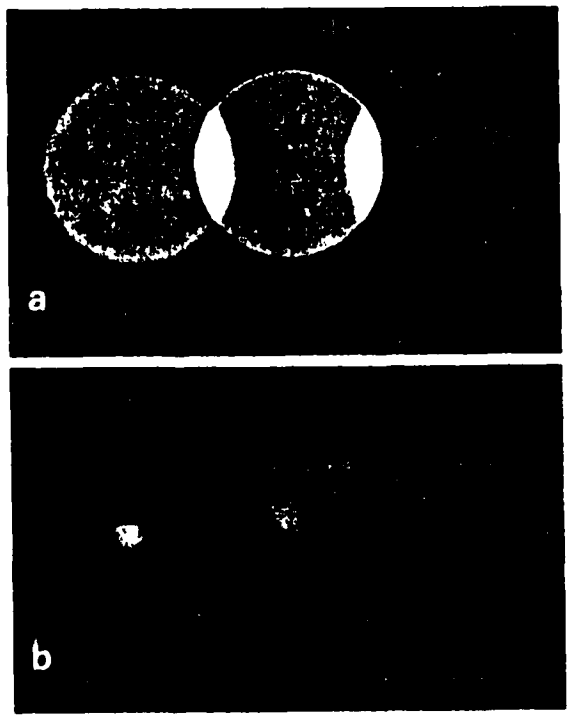


Fig. 5. Restoration of three defocused color point spread functions. a) A black-and-white photograph of three overlapping primary color disks as the color defocused point spread functions. b) A black-and-white photograph of the corresponding deblurred point spread functions.

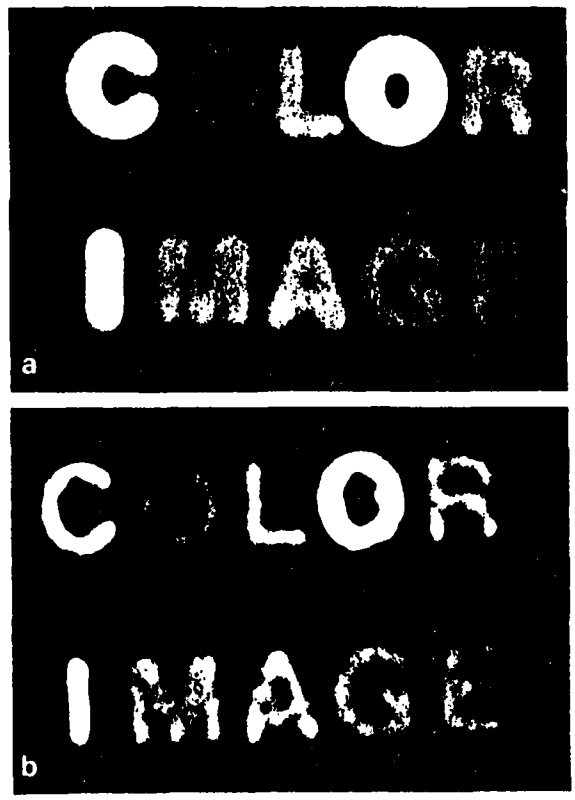


Fig. 6. Color image restoration of defocused color words "Color Image". a) A black-and-white photograph of the defocused color words. b) A black-and-white photograph of the corresponding deblurred color image.

relatively temporally broad and spatially large primary color light sources, the finger print like structure coherent artifact noise is eliminated, as can be seen from figs. 3b, 5b, and 6b.

## 4. Summary

We have shown that the color image restoration for out-of-focused photographic images can be obtained by a white-light processing technique. This technique uses a diffraction grating to generate three diffraction orders, so that three relatively spectrally broad and spatially large primary color sources can be derived from these diffractions. Since the temporal and spatial coherence requirements for the image deblurring are determined by the spectral bandwidth and the spatial size of the primary color sources, the three primary color partially coherent sources can be obtained by this proposed technique. The advantage of the technique is that one can adjust the degree of the temporal and spatial coherence of each primary color source by simply changing its diameter. By utilizing these primary color sources, an out-of-focused blurred color photographic image can be restored by a set of color sensitive inverse filters. And good deblurred color images have been obtained with pinhole sizes as large as 400 $\mu$m. To alleviate the low diffraction efficiency of the holographic inverse filters, the filter synthesis are obtained by the combination of non-absorptive phase filters and absorptive amplitude filters. The phase filters are obtained with a bleaching technique, while the amplitude filters are obtained by intensity exposure.

In view of the experimental results, we see that the resolved color images offer a reasonably good deblurred image quality and the colors are faithfully reproduced. Since the primary color light sources are spectrally and spatially broad, the coherent artifact noise is substantially suppressed. Although there is some degree of chromatic aberration, it can be alleviated by utilizing higher quality achromatic transform lenses.

We acknowledge the support of the U.S. Air Force Office of Scientific Research Grant AFOSR-81-0148.

## References

[1] J. Tsujiuchi, Correction of optical image by compensation of aberration and spatial frequency filtering, in: Progress in Optics, Vol. II, ed. E. Wolf (North-Holland Publishing Company, Amsterdam, 1963) p. 133.
[2] G.W. Stroke and R.G. Zech, Phys. Lett. A25 (1967) 89.
[3] J. Tsujiuchi, T. Honda and T. Fukaya, Optics Comm. 1 (1970) 379.
[4] [illegible] Horner, J. Opt. Soc. Am. 59 (1969) 553.
[5] [illegible] Horner, Appl. Optics 9 (1970) 167.
[6] X.J. [illegible], Optics and Fine Mechanics 10 (1977) 302, (chinese journal).
[7] R.M. Vasu and G.L. Rogers, Appl. Optics 19 (1980) 469.
[8] G.G. Yang and E.N. Leith, Optics Comm. 36 (1981) 101.
[9] F.T.S. Yu, Appl. Optics 17 (1978) 3571.
[10] S.L. Zhuang, T.H. Chao and F.T.S. Yu, Optics Lett. 6 (1981) 102.
[11] F.T.S. Yu, S.L. Zhuang and T.H. Chao, J. Optics (Paris) 13 (1982) 57.
[12] T.H. Chao, S.L. Zhuang, S.Z. Mao and F.T.S. Yu, Appl. Optics, to be published.
[13] M. Born and E. Wolf, Principles of optics, 2nd rev. ed. (Pergamon Press, New York, 1964) chapter 10.
[14] S.L. Zhuang and F.T.S. Yu, Appl. Optics 21 (1982) 2587.

# SECTION VII

## Source Encoding, Sampling and Spectral Band Filtering

Original article

*J. Optics (Paris)*, 1983, vol. *14*, n° 4, pp. 173-178

ELECTRICAL ENGINEERING DEPARTMENT
THE PENNSYLVANIA STATE UNIVERSITY

*University Park, Pennsylvania 16802*

# SOURCE ENCODING, SIGNAL SAMPLING AND SPECTRAL BAND FILTERING FOR PARTIALLY COHERENT OPTICAL SIGNAL PROCESSING

F. T. S. YU

MOTS CLÉS
Traitement optique
Cohérence

KEY WORDS
Optical processing
Coherence

SUMMARY : Relations between coherence requirement, spectral filtering, signal sampling, and source encoding are discussed. Since the spatial coherence requirement is determined by the signal processing operation, a strict spatial coherence is usually not required. The advantage of the source encoding is to relax the constraints of a physical light source so that the signal processing can be carried out with an extended incoherent source. The effect of signal sampling is to improve the temporal coherence requirement at the Fourier plane so that the spatial filtering can be carried out with partially coherence mode. The objective of broad spectral band filtering is to carry out the signal processing over the entire spectral band of the light source so that the coherent noise can be eliminated. Since the partially coherent optical processor utilizes a broad spectral band white-light source, it is particularly suitable for color signal processing. Experimental demonstrations for the source encoding, signal sampling and spectral band filtering are included.

**Traitement optique en éclairage partiellement cohérent en modulant la source et le signal et en filtrant le spectre du signal**

RÉSUMÉ : On discute des relations entre la cohérence, le filtrage, l'échantillonnage du signal et la modulation de la source. Puisque le degré de cohérence spatiale est déterminé par le traitement de l'image, une parfaite cohérence spatiale n'est, en général, pas nécessaire. L'avantage de moduler la source est de permettre de traiter l'image avec une source étendue incohérente. L'effet d'échantillonner l'image est d'améliorer la cohérence temporelle dans le plan de Fourier de façon que le filtrage puisse s'effectuer en lumière partiellement cohérente temporellement. L'utilisation d'un domaine spectral large a pour but de réduire le bruit dû à la cohérence spatiale de l'éclairage. Enfin, puisque un dispositif de traitement d'image en lumière partiellement cohérente utilise une source de lumière blanche, il paraît particulièrement bien adapté au traitement des images en couleurs. On présente des expériences montrant l'avantage de moduler la source et d'échantillonner l'image lorsqu'on utilise une source étendue de lumière blanche.

## *INTRODUCTION*

Since the invention of laser (i.e., a strong coherent source) laser has become a fashionable tool for many scientific applications particularly as applied to coherent optical signal processing. However coherent optical signal processing systems are plagued with coherent noises, which frequently limit their processing capability. As noted by the late Gabor, the Nobel prize winner in physics in 1970 for his invention of holography, the coherent noise is the number one enemy of the Modern Optical Signal Processing [1]. Aside the coherent noise, the coherent sources are usually expensive, and the coherent processing environments are very stringent. For example, heavy optical benches and dust free environments are generally required.

Recently, we have looked at the optical processing from a different standpoint. A question arises, is it necessarily true that all optical signal processing required a coherent source ? The answer to this question is that there are many optical signal processings that can be carried out by a white-light source [2]. The advantages of the proposed white-light signal processing technique are : 1. It is capable of suppressing the coherent noise; 2. White-light sources are usually inexpensive; 3. The processing environments are not critical; 4. The white-light sys-

tem is relatively easy and economical to maintain; and 5. The white-light processor is particularly suitable for color image processing.

One question that the reader may ask, since the white-light system offers all these glamorous merits, why it has been ignored for so long ? The answer to this question is that, it was a general acceptance that an incoherent source cannot process the signal in complex amplitude. However, none of the practical sources are strictly incoherent, even a white-light source. In fact, we were able to utilize the partial coherence of a white-light source to perform the complex amplitude processing. The proposed white-light processor, on one hand it is capable of suppressing the coherent noise like an incoherent processor, on the other hand it is capable of processing the signal in complex amplitude like a coherent processor.

There is however a basic different approach toward a coherent and a white-light processor. In coherent processing, virtually no one seems to care about the coherence requirements, since the laser provides a strong coherent source. However, in white-light processing, the knowledge of the coherence requirement is usually needed.

In white-light processing we would approach the problem backward. First, we should know what is the processing operation we wish to perform : Is it a 1-*D* or 2-*D* processing ? Is the signal filtering a point or point-pair concept ? What is the spatial bandwidth of the signal ? etc. Then with these knowledges, we would be able to evaluate the coherence requirements at the Fourier and at the input planes. From the evaluated results, we would be able to design a signal sampling function and a source encoding function to obtain these requirements. The objective of using a signal sampling function is to achieve a high degree of temporal coherence in Fourier plane so that the signal can be processing in complex amplitude, for the entire spectral band of a white-light source. And for the source encoding is to alleviate the constraint of an extended white-light source.

In the following sections, we shall discuss in detail the source encoding, signal sampling and spatial band filtering as applied to a partially coherent optical (e.g., white-light) signal processing.

## PARTIALLY COHERENT OPTICAL SIGNAL PROCESSING

We shall now describe an optical signal processing technique that can be carried out by a broad band white-light source, as illustrated in *figure 1*. The white-light signal processing system is similar to that of a coherent system, except the use of a white-light source, source encoding mask, signal sampling grating, multispectral filters and achromatic transform lenses. For example, if we place a signal transparency $s(x, y)$ in contact with a sampling phase grating, the complex light field for every wavelength $\lambda$ behind the achromatic transform lens $L_1$ would be

$$E(p, q; \lambda) = \iint s(x, y) \exp(i p_0 x) \times \times \exp[-i(px + qy)]\, dx\, dy = S(p - p_0, q), \quad (1)$$

where the integral is over the spatial domain of the input plane $P_1$. $(p, q)$ denotes the angular spatial frequency coordinate system, $p_0$ is the angular spatial frequency of the sampling phase grating, and $S(p, q)$ is the Fourier spectrum of $s(x, y)$. If we write Eq. (1) in the form of linear spatial coordinate system $(\alpha, \beta)$, we have

$$E(\alpha, \beta; \lambda) = S\left(\alpha - \frac{\lambda f}{2\pi} p_0, \beta\right), \quad (2)$$

where $p \triangleq (2\pi/\lambda f)\,\alpha$, $q \triangleq (2\pi/\lambda f)\,\beta$, and $f$ is the focal length of the achromatic transform lens. Thus, we see that the Fourier spectra would disperse into rainbow color along the $\alpha$ axis, and each Fourier spectrum for a given wavelength $\lambda$ is centered at $\alpha \pm (\lambda f/2\pi)\, p_0$.

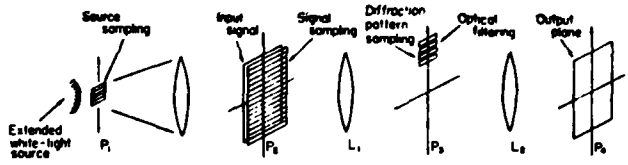


FIG. 1. — *A white-light optical signal processor.*

*In signal filtering, we assume that a sequence of* complex spatial filters for various $\lambda_n$ are available, i.e., $H(p_n, q_n)$, where $p_n = (2\pi/\lambda_n f)\,\alpha$, $q_n = (2\pi/\lambda_n f)\,\beta$. In practice, all the processing signals are spatial frequency limited, the spatial bandwidth of each spectral band filter $H(p_n, q_n)$ is also bandlimited, such as

$$H(p_n, q_n) = \begin{cases} H(p_n, q_n), & \alpha_1 < \alpha < \alpha_2, \\ 0, & \text{otherwise}, \end{cases} \quad (3)$$

where $\alpha_1 \triangleq (\lambda_n f/2\pi)(p_0 + \Delta p)$ and $\alpha_2 = (\lambda_n f/2\pi) \times (p_0 - \Delta p)$ are the upper and the lower spatial limits of $H(p_n, q_n)$, and $\Delta p$ is the spatial bandwidth of the input signal $s(x, y)$.

The limiting wavelengths of each $H(p_n, q_n)$ can be written as

$$\lambda_l = \lambda_n \frac{p_0 + \Delta p}{p_0 - \Delta p}, \quad \text{and} \quad \lambda_h = \lambda_n \frac{p_0 - \Delta p}{p_0 + \Delta p}. \quad (4)$$

The spectral bandwidth of $H(p_n, q_n)$ is therefore,

$$\Delta\lambda_n = \lambda_n \frac{4 p_0 \Delta p}{p^2 - (\Delta p)^2} \simeq \frac{4 \Delta p}{p_0} \lambda_n. \quad (5)$$

If we place this set of spectral band filters side-by-side positioned over the smeared Fourier spectra, then the intensity distribution of the output light field can be shown as,

$$I(x, y) \simeq \sum_{n=1}^{N} \Delta\lambda_n \left| s(x, y; \lambda_n) * h(x, y; \lambda_n) \right|^2, \quad (6)$$

where $h(x, y; \lambda)$ is the spatial impulse response of

$H(p_n, q_n)$ and * denotes the convolution operation. Thus, the proposed white-light signal processor is capable of processing the signal in complex amplitude. Since the output intensity is the sum of the mutually incoherent narrow band irradiances, the annoying coherent noise can be eliminated. Furthermore, the white-light source contains all the color wavelengths, the proposed system is particularly suitable for color signal processing.

## SPECTRAL BAND FILTERING, SIGNAL SAMPLING AND SOURCE ENCODING

We have mentioned earlier for white-light or partially coherent processing, we would approach the problem in backward manner. For example, if signal filtering is two-dimensional (e.g., 2-D correlation operation), we would synthesize a set of narrow spectral band filters for each $\lambda_n$ for the entire smeared Fourier spectra, as illustrated in *figure 2(a)*. On the other hand, if the signal filtering is one-dimensional (e.g., deblurring due to linear motion), a broadband fan-shape spatial filter, to accomodate the scale variation due to wavelength, can be utilized as illustrated in *figure 2(b)*. Since the filtering is taken place with the entire spectral band of the light source, the coherent noise can be suppressed and the white-light processing technique is very suitable for colour image processing.

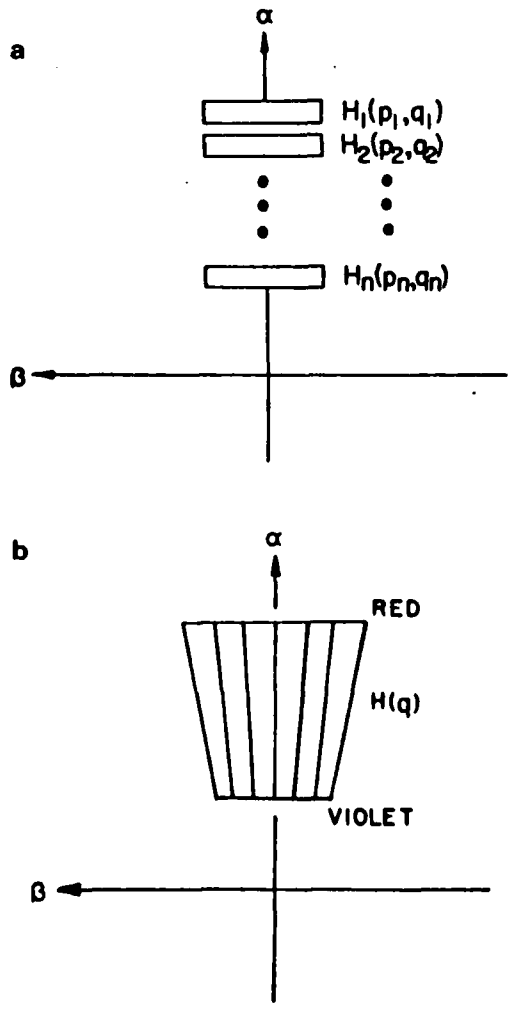


FIG. 2. — (a) *A multi spectral-band filter.* (b) *A fan-shape filter.*

There is, however, a temporal coherence requirement imposed upon the signal filtering in Fourier plane. Since the scale of the Fourier spectrum varies with wavelength, a temporal coherence requirement should be imposed on each spatial filter at the Fourier plane. Thus, the spectral spread over each filter $H(p_n, q_n)$ is imposed by the temporal coherence requirement, i.e.,

$$\frac{\Delta\lambda_n}{\lambda_n} = \frac{4\,\Delta p}{P_0} \ll 1 . \tag{7}$$

From this requirement, a high degree of temporal coherence is achievable in the Fourier plane by simply increasing the spatial frequency of the sampling grating. Needless to say that the same temporal coherence requirement of Eq. (7) can also be applied for a broadband fan-shape filter.

There is also a spatial coherence requirement imposed at the input plane of the white-light processor. With reference to the Wolf's [3] partial coherence theory [3], the spatial coherence function at the input plane can be shown [4],

$$\Gamma(\mathbf{x} - \mathbf{x}') = \iint \gamma(\mathbf{x}_0) \exp\left[ i\,2\,\pi \frac{\mathbf{x}_0}{\lambda f}(\mathbf{x} - \mathbf{x}') \right] d\mathbf{x}_0 , \tag{8}$$

where $\gamma(\mathbf{x}_0)$ denotes the intensity distribution of the source encoding function.

From the above equation, we see that the spatial coherence and source encoding functions form a Fourier transform pair, i.e.,

$$\gamma(\mathbf{x}_0) = \mathcal{F}[\Gamma(\mathbf{x} - \mathbf{x}')] , \tag{9}$$

and

$$\Gamma(\mathbf{x} - \mathbf{x}') = \mathcal{F}^{-1}[\gamma(\mathbf{x}_0)] , \tag{10}$$

where $\mathcal{F}$ denotes the Fourier transformation. This Fourier transform pair implies that if a spatial coherence function is given then the source encoding function can be evaluated through the Fourier transformation and vice versa. We note that source encoding function can consist of apertures of any shape or complicated gray scale transparency. However the source encoding function is only limited to a positive real quantity which is restricted by the following physical realizable condition :

$$0 \leq \gamma(\mathbf{x}_0) \leq 1 . \tag{11}$$

In white-light processing, we would search for a reduced spatial coherence requirement for the processing operation. With reference to this reduced spatial coherence function, a source encoding function that satisfied the physical realizability condition can be obtained. One of the basic objectives of the source encoding is to alleviate the constraint of a white-light source. Furthermore the source encoding also improves the utilization of the light power such that the optical processing can be carried out by an extended source.

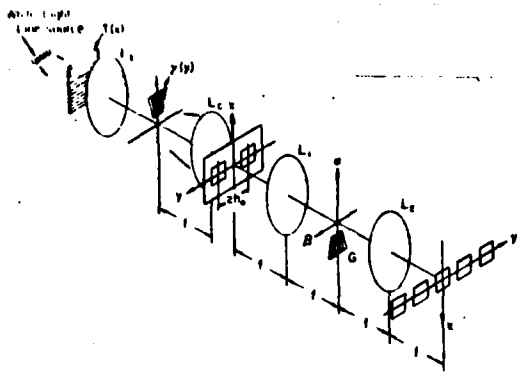

FIG. 3. — *A white-light image subtraction processor. T(x) : phase grating. $L_1$ : image lens. $L_C$ : collimated lens. $L_1$ and $L_2$ : achromatic transform lenses. γ(y), source encoding mask. G : fan-shape diffraction grating.*

We shall now illustrate an application of the source encoding, signal sampling and filtering for a white-light signal processing. Let us now consider a polychromatic image subtraction [5]. The image subtraction of Lee [6] that we would consider is essentially a one-dimensional processing operation, in which a 1-*D* fan-shape diffraction grating should be utilized, as illustrated in *figure 3*. We note that the fan-shape grating (i.e., filter) is imposed by the temporal coherence condition of Eq. (7). Since the image subtraction is a point-pair processing operation, a strictly broad spatial coherence function at the input plane is not required. In other words, if one maintains the spatial coherence between the corresponding image points to be subtracted at the input plane, then the subtraction operation can be carried out at the output image plane. Thus instead of using a strictly broad spatial coherence function, a reduced spatial coherence function may be utilized, such as

$$\Gamma(y - y') = \delta(y - y' - h_0) + \delta(y - y' + h_0), \quad (12)$$

where $2h_0$ is the main separation between the two input color transparencies. The source encoding function can therefore be evaluated by through the Fourier transform of Eq. (9), such as

$$\gamma(y_0) = 2\cos\left(\frac{2\pi h_0}{\lambda f} y_0\right). \quad (13)$$

Unfortunately Eq. (13) is a bipolar function which is not physically realizable. To ensure a physically realizable source encoding function, we let a reduced spatial coherence function with the required point-pair coherence characteristic be [7].

$$\Gamma(|y - y'|) = \frac{\sin\left(\frac{N\pi}{h_0}|y - y'|\right)}{N\sin\left(\frac{\pi}{h_0}|y - y'|\right)} \operatorname{sinc}\left(\frac{\pi w}{h_0 d}|y - y'|\right), \quad (14)$$

where $N \gg 1$ a positive integer, and $w \ll d$. Eq. (14) represents a sequence of narrow pulses which occur at every $|y - y'| = nh_0$, where $n$ is a positive integer, and their peak values are weighted by a broader sine factor, as shown in *figure 4(a)*. Thus, a high degree of spatial coherence can be achieved at every point-pair between the two input color transparencies. By taking the Fourier transformation of the reduced spatial coherence function of Eq. (14), the corresponding source encoding function is

$$\gamma(|y|) = \sum_{n=1}^{N} \operatorname{rect}\frac{|y - nd|}{w}, \quad (15)$$

where $w$ is the slit width, $d = (\lambda f/h_0)$ is the separation between the slits, and $N$ is the number of the slits. Since $\gamma(|y|)$ is a positive real function which satisfies the constraint of Eq. (11), the proposed source encoding function of Eq. (15) is physically realizable.

In view of Eq. (15), we also note that, the separation of slit $d$ is linearly proportional of the $\lambda$. The source encoding is a fan-shape type function, as shown in *figure 4(b)*. To obtain lines of rainbow color spectral light source for the signal processing, we would utilize a linear extended white-light source with a dispersive phase grating, as illustrated in *figure 3*. Thus with

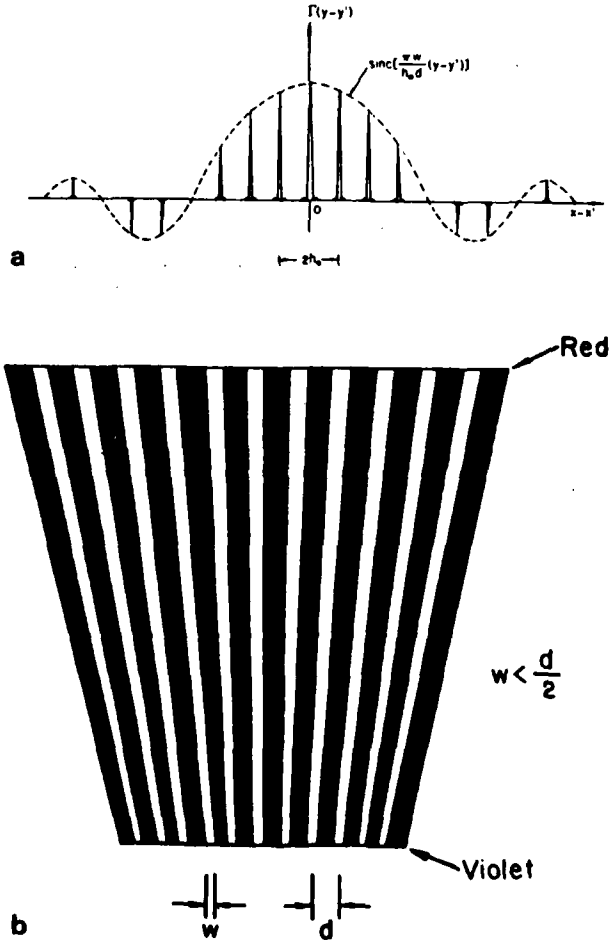


FIG. 4. — (a) *A spatial coherence function.* (b) *A source encoding mask.*

a b

FIG. 5. — (a) *A blurred color image.* (b) *A deblurred color image.*

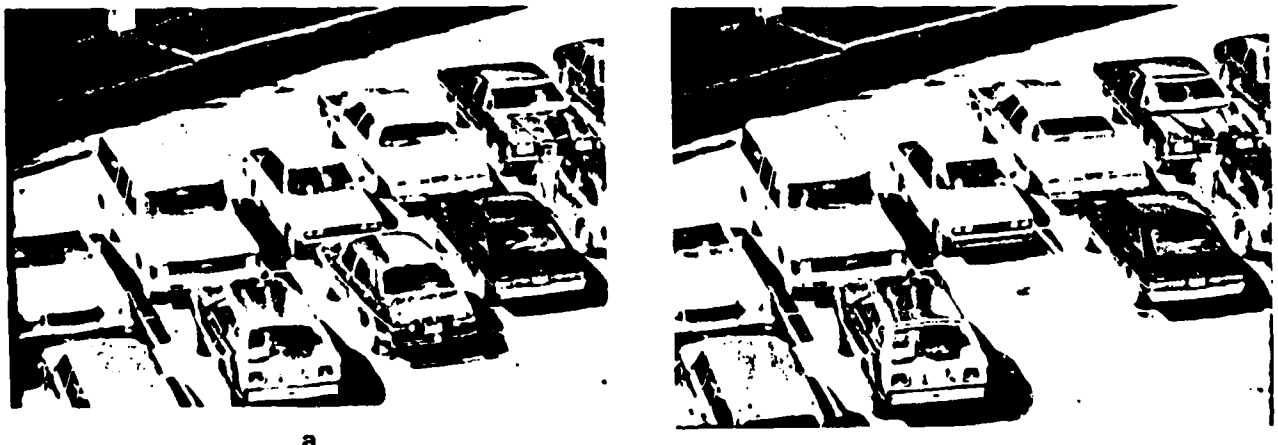

a b

c

FIG. 6. — (a) *and* (b). *Pictures of the input color objects.* (c) *The subtracted color image.*

appropriate source encoding, signal sampling and filtering, color image subtraction operation can be obtained at the output plane. We stress again, the basic advantage of source encoding is to alleviate the constraint of strict spatial coherence requirement imposed upon the optical signal processor. The source encoding also offers the advantage of efficient utilization of the light power.

## EXPERIMENTAL DEMONSTRATIONS

We shall now provide a couple of experimental results obtained with the source encoding, signal sampling and spectral band filtering technique for white-light and extended incoherent courses. We shall first show the result obtained for color image deblurring due to linear motion with the white-light processing technique. Since linear motion deblurring is a 1-D processing operation and the inverse filtering is a point-by-point filtering concept such that the operation is taking place on the smearing length of the blurred image. Thus the deblurring filter (i.e., inverse filter) is a fan-shape type spatial filter [8] and the temporal coherence requirement is imposed by Eq. (7). The spatial coherence requirement is dependent upon the smearing length. A source encoding function of a narrow slit width (dependent upon the smearing) perpendicular to the smearing length is utilized. *Figure 5(a)* shows a color picture of a blurred image due to linear motion of a F-16 fighter plane. The body of this fighter plane is painted in navy blue-and-white colors, the wings are mostly painted in red, the tail is navy blue-and-white, and the ground terrain is generally bluish color. From this figure, we see that the plane is badly blurred. *Figure 5(b)* shows the color image deblurring result that we obtained with the proposed white-light deblurring technique. From this deblurred result, the letters and overall shape of the entire airplane are more distinctive than the blurred one. Furthermore the river, the highways, and the forestry of the ground terrain are far more visible. We note that the color reproduction of the deblurred image is spectacularly faithful, and coherent artifact noise is virtually non-existed. There is, however, some degree of color blur and color deviation, which are primarily due to the chromatic aberration and the anti-reflectance coating of the transform lenses. Nevertheless, these drawbacks can be overcome by utilizing good quality achromatic transform lenses.

Let us now provide a color image subtraction utilized by the source encoding technique with extended incoherent sources as described in previous sections. *Figure 6(a)* and *6(b)* show two color image transparencies of a parking lot as input color objects. *Figure 6(c)* shows the color subtracted image obtained by the source encoding technique with extended incoherent source. In this figure, the profile of a (red) subcompact car can be seen at the output image plane. The shadow and the parking line (in yellow color) can also be readily identified. We however note that, this color image subtraction result is obtained by two narrow band extended incoherent sources. Extention toward the entire spectral band of a white-light source is currently under investigation.

## CONCLUSION

In conclusion we would point out that the advantage of source encoding is to provide an appropriate spatial coherence function at the input plane so that the signal processing can be carried out by an extended incoherent source. The effect of the signal sampling is to achieve the temporal coherence requirement at the Fourier plane so that the signal can be processed in complex amplitude. If the filtering operation is two-dimensional, a multi-spectral-band 2-*D* filters should be utilized. If the filtering operation is one-dimensional, a fan-shape filter can be used.

In short, one should carry out the processing requirements backward for a partially coherent or white-light processing. With these processing requirements (e.g., operation, temporal and spatial coherence requirements), multi-spectral-band or fan-shape filter, signal sampling function, and source encoding mask can be synthesized. Thus the signal processing can be carried out in complex amplitude over the whole-spectral band of an extended white-light source.

We acknowledge the support of the U.S. Air Force Office of Scientific Research Grant AFOSR-81-0148.

* * *

## *REFERENCES*

[1] Gabor (D.). – IBM. J. Res. Develop. 1970, *14*, 509.

[2] Yu (F. T. S.). – Optical Information Processing, Wiley-Interscience, NY, 1983.

[3] Born (M.) and Wolf (E.). – *Principles of Optics*, 2nd rev. ed., Pergamon Press, New York, 1964.

[4] Yu (F. T. S.), Zhuang (S. L.) and Wu (S. T.). – *Appl. Phys.*, 1982, *B27*, 99.

[5] Yu (F. T. S.) and Wu (S. T.). – *J. Opt.*, 1982, *13*, 183.

[6] Lu (S. H.), Yao (S. K.) and Muns (A. G.). – *J. Opt. Soc. Am.*, 1970, *60*, 1037.

[7] Wu (S. T.) and Yu (F. T. S.). – *Appl. Opt.*, 1981, *20*, 4082.

[8] Chao (T. H.), Zhuang (S. L.), Mao (S. Z.) and Yu (F. T. S.). – *Appl. Opt.*, 1983, *22*, 1439.

*(Manuscript received in March, 7, 1983.)*

# SECTION VIII

## Advances in White-Light Signal Processing

# ADVANCES IN WHITE-LIGHT OPTICAL SIGNAL PROCESSING*

F. T. S. Yu
Electrical Engineering Department
The Pennsylvania State University
University Park, Pennsylvania 16802

## SUMMARY

A technique that permits signal processing operations to be carried out by white-light source is described. This method is capable of performing signal processing that obeys the concept of coherent light rather than incoherent optics. Since the white-light source contains all the color wavelengths of the visible light, the technique is very suitable for color signal processing. Some of its recent advances in white-light signal processing will be illustrated.

## INTRODUCTION

The use of coherent light enables optical systems to carry out many sophisticated information processing operations (ref. 1). However, coherent optical processing systems are plagued with coherent artifact noise, which frequently limits their processing capability. Although many optical information processing operations can be implemented by systems that use incoherent light (refs. 2-5), there are other severe drawbacks. The incoherent processing system is capable of reducing the inevitable artifact noise, but it generally introduces a dc-bias buildup problem, which results in poor noise performance. Techniques have been developed for coherent operation with light of reduced coherence (refs. 6,7); however, these techniques also possess severe limitations.

Attempts at reducing the temporal coherence requirements on the light source in optical information processing fall into two general categories: one, the use of incoherent instead of coherent optical processing has been pursued by Lowenthal and Chavel (ref. 8) and Lohmann (ref. 9), among others. The other, the reduction of coherence while still operating in the linear-in-amplitude, has been pursued by Leith and Roth (ref. 10) and by Morris and George (ref. 11).

Since the invention of laser (i.e., a strong coherent source), it has become a fashionable tool for many scientific applications particularly as applied to coherent optical signal processing. However coherent optical signal processing systems are plagued with coherent noises, which frequently limit their processing capability. As noted by the late Gabor, the Nobel prize winner in physics in 1970 for his invention of holography, the coherent noise is the number one enemy of the Modern Optical Signal Processing (ref. 12). Aside from the coherent noise, the coherent sources are usually expensive, and the coherent processing environments are very stringent. For example, heavy optical benches and dust free environments are generally required.

Recently, we have looked at the optical processing from a different standpoint. A question arises, is it necessarily true that all optical signal processing required

*This research is supported in part by the Air Force Office of Scientific Research.

a coherent source? The answer to this question is that there are many optical signal processings that can be carried out by a white-light source (ref. 13). The advantages of the proposed white-light signal processing technique are: 1. It is capable of suppressing the coherent noise; 2. White-light source is usually inexpensive; 3. The processing environment is not very demanding; 4. The white-light system is relatively easy and economical to maintain; and 5. The white-light processor is particularly suitable for color image processing.

One question that the reader may ask, since the white-light system offers all these glamorous merits, is why has it been ignored for so long? The answer to this question is that it was a general acceptance that an incoherent source cannot process the signal in complex amplitude. However, none of the practical sources are strictly incoherent, even a white-light source. In fact, we were able to utilize the partial coherence of a white-light source to perform the complex amplitude processing. The proposed white-light processor, on one hand, is capable of suppressing the coherent noise like an incoherent processor, and on the other hand, it is capable of processing the signal in complex amplitude like a coherent processor.

There is however a different approach toward the utilization of a white-light processor. In coherent processing, virtually no one evaluates the coherence requirement, since the laser provides a very good coherent source. However, in white-light processing, the evaluation of the coherence requirement is usually called for.

In white-light signal processing we should approach the problem from a different standpoint. First, we should have the a priori knowledge of the signal processing operation we would encounter. For example, is it a 1-D or 2-D processing? Is the signal filtering a point or point-pair concept? What is the spatial bandwidth of the signal? Then we would be able to evaluate the coherence requirements at the Fourier and at the input planes. From the evaluated results, we would be able to design a signal sampling function and a source encoding mask to obtain these requirements. The objective of using a signal sampling function is to achieve a high degree of temporal coherence in Fourier plane so that the signal can be processed in complex amplitude for the entire spectral band of the light source. And for the source encoding, it is to alleviate the inability of an extended source.

In the following, we shall discuss in detail the source encoding, signal sampling and spatial band filtering as applied to white-light signal processing.

## WHITE-LIGHT OPTICAL SIGNAL PROCESSING

We shall now describe an optical signal processing technique that can be carried out by a white-light source, as illustrated in Fig. 1. The white-light signal processing system is similar to that of a coherent system, except for the use of a white-light source, source encoding mask, signal sampling grating, multispectral filters and achromatic transform lenses. For example, if we place a signal transparency $s(x,y)$ in contact with a sampling phase grating, the complex light field for every wavelength $\lambda$ behind the achromatic transform lens $L_1$ would be

$$E(p,q;\lambda) = \iint s(x,y)\, \exp(ip_o x)\exp[-i(px+qy)]dxdy = S(p-p_o,q) \qquad (1)$$

where the integral is over the spatial domain of the input plane $P_1$, $(p,q)$ denotes the angular spatial frequency coordinate system, $p_o$ is the angular spatial frequency

of the sampling phase grating, and $S(p,q)$ is the Fourier spectrum of $s(x,y)$. If we write Eq. (1) in the form of linear spatial coordinate system $(\alpha,\beta)$, we have,

$$E(\alpha,\beta;\lambda) = S(\alpha - \frac{\lambda f}{2\rho} p_o, \beta) \tag{2}$$

where $p = (2\pi/\lambda f)\alpha$, $q = (2\pi/\lambda f)\beta$, and f is the focal length of the achromatic transform lens. Thus, we see that the Fourier spectra would disperse into rainbow color along the $\alpha$ axis, and each Fourier spectrum for a given wavelength $\lambda$ is centered at $\alpha = \pm(\lambda f/2\pi)p_o$.

In signal filtering, we assume that a sequence of complex spatial filters for various $\lambda_n$ are available, i.e., $H(p_n,q_n)$, where $p_n = (2\pi/\lambda_n f)\alpha$, $q_n = (2\pi/\lambda_n f)\beta$. In practice, all the processing signals are spatial frequency limited; the spatial bandwidth of each spectral band filter $H(p_n,q_n)$ is also bandlimited, such as

$$H(p_n,q_n) = \begin{cases} H(p_n,q_n), \alpha_1 < \alpha < \alpha_2 \\ 0, \quad \text{otherwise} \end{cases} \tag{3}$$

where $\alpha_1 = (\lambda_n f/2\pi)(p_o + \Delta p)$ and $\alpha_2 = (\lambda_n f/2\pi)(p_o - \Delta p)$ are the upper and the lower spatial limits of $H(p_n,q_n)$, and $\Delta p$ is the spatial bandwidth of the input signal $s(x,y)$.

The limiting wavelengths of each $H(p_n,q_n)$ can be written as

$$\lambda_\ell = \lambda_n \frac{p_o + \Delta p}{p_o - \Delta p}, \text{ and } \lambda_h = \lambda_n \frac{p_o - \Delta p}{p_o + \Delta p} \tag{4}$$

The spectral bandwidth of $H(p_n,q_n)$ is therefore

$$\Delta\lambda_n = \lambda_n \frac{4p_o\Delta p}{p^2 - (\Delta p)^2} \simeq \frac{4\Delta p}{p_o} \lambda_n \tag{5}$$

If we place this set of spectral band filters side-by-side positioned over the smeared Fourier spectra, then the intensity distribution of the output light field can be shown as

$$I(x,y) \simeq \sum_{n=1}^{N} \Delta\lambda_n \left| s(x,y;\lambda_n) * h(x,y;\lambda_n) \right|^2 \tag{6}$$

where $h(x,y;\lambda)$ is the spatial impulse response of $H(p_n,q_n)$ and * denotes the convolution operation. Thus, the proposed white-light signal processor is capable of processing the signal in complex amplitude. Since the output intensity is the sum of the mutually incoherent narrow band spectral irradiances, the annoying coherent artifact can be eliminated. Furthermore, the white-light source contains all the color wavelengths; the processor is very suitable for color signal processing.

As stated earlier, in white-light signal processing we would approach the problem from a different standpoint. For example, if signal filtering is two-dimensional (e.g., 2-D correlation operation), we would synthesize a set of narrow spectral band filters for each $\lambda_n$ for the entire smeared Fourier spectra, as illustrated in Fig. 2(a). On the other hand, if the signal filtering is one-dimensional (e.g., deblurring due to linear motion), a broadband fan-shape spatial filter, to accommodate the scale variation due to wavelength, can be utilized as illustrated in Fig. 2(b). Since the filtering is taking place with the entire spectral band of the light source, the artifact noise can be suppressed and the white-light processing technique is also suitable for color image processing.

There is, however, a temporal coherence requirement imposed upon the signal filtering in Fourier plane. Since the scale of the Fourier spectrum varies with wavelength, a temporal coherence requirement should be imposed on each spatial filter at the Fourier plane. Thus, the spectral spread over each filter $H(p_n,q_n)$ is imposed by the temporal coherence requirement, i.e.,

$$\frac{\Delta\lambda_n}{\lambda_n} = \frac{4\Delta p}{p_o} << 1 \tag{7}$$

From this inequality, a high degree of temporal coherence is achievable in the Fourier plane by simply increasing the spatial frequency of the sampling grating. Needless to say, the same tempoal coherence requirements of Eq. (7) can also be applied for a broadband fan-shape filter.

There is also a spatial coherence requirement imposed at the input plane of the white-light signal processor. The spatial coherence function at the input plane can be shown (refs. 14,15),

$$\Gamma(\vec{x}-\vec{x}') = \int\int \gamma(\vec{x}_o)\exp[i2\pi \frac{\vec{x}_o}{\lambda f}(\vec{x}-\vec{x}')]d\vec{x}_o \tag{8}$$

which essentially is the Van Cittert-Zernike Theorem (refs. 16,17), where $\gamma(\vec{x}_o)$ denotes the intensity distribution of the source encoding function.

From the above equation, we see that the spatial coherence and source encoding functions form a Fourier transform pair, i.e.,

$$\gamma(\vec{x}_o) = \mathcal{F}[\Gamma(\vec{x}-\vec{x}')] \tag{9}$$

and

$$\Gamma(\vec{x}-\vec{x}') = \mathcal{F}^{-1}[\gamma(\vec{x}_o)] \tag{10}$$

where $\mathcal{F}$ denotes the Fourier transformation. This Fourier transform pair implies that if a spatial coherence function is given then the source encoding function can be determined with the Fourier transformation and vice versa. We note that source encoding function can consist of apertures of any shape or complicated gray scale

transmittance. However the source encoding function is only limited to a positive real quantity which is restricted by the following physical realizable condition:

$$0 \leq \gamma(\vec{x}_o) \leq 1 \tag{11}$$

In white-light signal processing, we would search for a reduced spatial coherence requirement for the processing operation. With reference to this reduced spatial coherence function, a source encoding function that satisfies the physical realizability condition can be obtained. One of the basic objectives of the source encoding is to alleviate the inability of a physical white-light source. Furthermore the source encoding also improves the utilization of the light power such that the optical processing can be carried out by an extended source.

We shall now illustrate an application of the source encoding, signal sampling, and filtering for a white-light signal processing. Let us now consider a polychromatic image subtraction (ref. 18). The image subtraction of Lee (ref. 19) that we would consider is essentially a one-dimensional processing operation, in which a 1-D fan-shape diffraction grating should be utilized, as illustrated in Fig. 3. We note that the fan-shape grating (i.e., filter) is imposed by the temporal coherence condition of Eq. (7). Since the image subtraction is a point-pair processing operation, a strictly broad spatial coherence function at the input plane is not required. In other words, if one maintains the spatial coherence between the corresponding image points to be subtracted at the input plane, then the subtraction operation can be carried out at the output image plane. Thus instead of using a strictly broad spatial coherence function, a reduced spatial coherence function may be utilized, such as

$$\Gamma(y-y') = \delta(y-y'-h_o) + \delta(y-y'+h_o) \tag{12}$$

where $2h_o$ is the main separation between the two input color transparencies. The source encoding function can therefore be evaluated by through the Fourier transform of Eq. (9), such as

$$\gamma(y_o) = 2\cos\left(\frac{2\pi h_o}{\lambda f} y_o\right) \tag{13}$$

Unfortunately Eq. (13) is a bipolar function which is not physically realizable. To ensure a physically realizable source encoding function, we let a reduced spatial coherence function with the point-pair coherence requirement be (ref. 20)

$$\Gamma(|y-y'|) = \frac{\sin\left(\frac{N\pi}{h_o}|y-y'|\right)}{N\sin\left(\frac{\pi}{h_o}|y-y'|\right)} \operatorname{sinc}\left(\frac{\pi w}{h_o d}|y-y'|\right) \tag{14}$$

where $N \gg 1$, a positive integer, and $w \ll d$. Equation (14) represents a seguence of narrow pulses which occur at every $|y-y'| = nh_o$, where n is a positive integer, and their peak values are weighted by a broader sinc factor, as shown in Fig. 4(a). Thus, a high degree of spatial coherence can be achieved at every point-pair between the two input color transparencies. By taking the Fourier transformation of the reduced spatial coherence function of Eq. (14), the corresponding source encoding

function is

$$\gamma(|y|) = \sum_{n=1}^{N} \text{rect}\,\frac{|y-nd|}{w} \qquad (15)$$

where w is the slit width, $d = (\lambda f/h_o)$ is the separation between the slits, and N is the number of the slits. Since $\gamma(|y|)$ is a positive real function which satisfies the constraint of Eq. (11), the proposed source encoding function of Eq. (15) is physically realizable.

In view of Eq. (15), we also note that the separation of slit d is linearly proportional to the $\lambda$. The source encoding is a fan-shape type function, as shown in Fig. 4(b). To obtain lines of rainbow color spectral light sources for the signal processing, we would utilize a linear extended white-light source with a dispersive phase grating, as illustrated in Fig. 3. Thus with the described broad-band source encoding mask, sampling grating, and fan-shape sinusoidal grating, a color substracted image can be seen at the output image plane.

## RECENT ADVANCES IN WHITE-LIGHT PROCESSING

It would occupy lengthy pages to describe most advances in white-light signal processing. We would however have to restrict our discussion to a few recent results that are considered interesting. Since the white-light signal processor is particularly suitable for color signal processing, we shall provide the results mostly in color images.

We shall first demonstrate a color image deblurring result due to linear motion. Since linear motion is a 1-D processing operation and its deblurring filter is a point-by-point filtering, a fan-shape deblurring filter can be utilized (ref. 21). Figure 5(a) shows a color picture of a blurred image due to linear motion of an F-16 fighter plane. The body of this fighter plane is painted in navy blue-and-white colors, the wings are mostly painted in red, the tail is also navy blue-and-white, and the ground terrain is generally bluish-green color. From this figure, we see that the plane is severely blurred due to motion. Figure 5(b) shows the color image deblurring result obtained with the white-light signal processing technique. From this result, the letters and overall shape of the entire airplane are more distinctive than the blurred one. The river, the highways, and the forestry of the ground terrain are far more visible. We note that the color reproduction of the deblurred image is spectacularly faithful and coherent artifact noise is virtually nonexistent.

Let us now provide a color image subtraction utilized by the source encoding technique with extended incoherent sources (ref. 18) as described in previous sections. Figure 6(a) and 6(b) show two color image transparencies of a parking lot as input color objects. Figure 6(c) shows the color subtracted image obtained by the source encoding technique with extended incoherent source. In this figure, the profile of a (red) subcompact car can be seen at the output image plane. The shadow and the parking line (in yellow color) can also be readily identified. However, we note that this color image subtraction result is obtained by two narrow spectral band extended incoherent sources. Extension toward the entire spectral band of a white-light source is currently under investigation.

We shall now illustrate our experimental result that a multicolor sound spectrogram (ref. 22) can be generated by a white-light processing technique, as illustrated in Fig. 7. Figure 8(a) shows a typical 1-D intensity modulated speech signal obtained by focusing its CRT scanner onto a moving photographic film by a film transport. If the recorded format transparency is transporting over a rectangular optical window at the input plane of Fig. 7, a frequency color encoded sound spectrogram can be recorded at the output plane. Figure 8(b) shows a typical frequency color coded speech spectrogram obtained with this technique. The frequency content is encoded from red for high frequency, green for intermediate frequency, to blue for low frequency. This color encoded speech spectrogram represents a sequence of English words spoken by a male voice. These words are "testing, one, two, three, four." From this color encoded speech spectrogram, we see that excellent characterization of format variation can readily be seen. Because of the use of a white-light source, the artifact noise is avoided. As compared with the electronic and digital counterparts, its white-light signal processing technique simplified the processing technology and the system is rather versatile to operate. Although the result provided is rather preliminary, it is the first color-coded speech spectrogram being generated.

We shall now illustrate a computer controlled white-light density pseudocolor encoder, as proposed in Fig. 9. The spatial encoding is made by multiplexing a positive, a negative, and a product image onto a black-and-white photographic film, as illustrated in Fig. 10. Figure 11 shows a sketch of the normalized transmittance as a function of gray scale. If the encoded transparency is inserted at the input plane of a white-light processor of Fig. 9, then a density color coded image can be obtained by color filtering at the Fourier plane.

We stress that this white-light pseudocolor encoder offers several advantages over the digital counterpart. The encoder is far less expensive and in principle the technique offers a higher image resolution.

Figure 12 shows a set color coded image of a woman's pelvis. The x-ray was taken following a surgical procedure. A section of the bone between the sacroiliac joint and spinal column has been removed. In Fig. 12(a), the positive image is encoded in red, the negative image is encoded in blue, and the product image is encoded in green. By comparing the pseudocolor coded image with the original black-and-white x-ray picture, it appears that the soft tissues can be better differentiated by the color images as demonstrated by the fact that the image contrast in the region containing the gastrointestinal tracts is evidently superior in the color image. On the other hand, there seems to be a degradation in the resolution in the color image along edges of the hard tissues. This is perhaps caused by two reasons: Firstly, high frequency information may be eliminated due to the low spatial frequency encoding gratings (40 lines/mm and 26.7 lines/mm) employed. Secondly, the image may be smeared due to the film development process. These two problems can be easily corrected by selecting higher frequency encoding gratings and by gaining more experience in film processing.

Another point worthwhile to note is that a reversal of the color encoding can be easily implemented as shown in Fig. 12(b), where the positive and negative images are encoded in blue and red while the product image remains in green. This color mixture capability could be beneficial because an image in different color combination may reveal subtle features which are otherwise undetected. For instance, the air pockets in the colon of the patient can be identified more easily with Fig. 12(b) than with Fig. 12(a). Moreover, a wide variety of other pseudocolor

encoded images can also be obtained by simply alternating the color filters in the Fourier plane of the white-light processor.

## CONCLUSION

In conclusion we would stress that source encoding is to provide an appropriate, reduced spatial coherence function at the input plane so that the signal processing can be carried out by an extended white-light source. The effect of the signal sampling is to achieve a higher temporal coherence at the Fourier plane so that the signal can be processed in complex amplitude. If the filtering operation is two-dimensional, a multi-spectral-band 2-D filters should be utilized. If the filtering operation is one-dimensional, a fan-shape filter can be used. In summary, the white-light signal processor is capable of processing the signal in complex amplitude as a coherent processor and, on the other hand, it suppresses the artifact noise as an incoherent processor. Since the white-light source contains all the visible wavelengths, it has been shown very suitable for color signal processing.

## REFERENCES


1. A. Vander Lugt, "Coherent Optical Processing," Proc. IEEE, 62, 1300 (1974).
2. G. L. Rogers, "Non-coherent Optical Processing," Opt. Laser Technol., 7, 153 (1975).
3. K. Bromley, "An Optical Incoherent Correlation," Opt. Acta, 21, 35 (1974).
4. M. A. Monahan, K. Bromley, and R. P. Bocker, "Incoherent Optical Correlations," Proc. IEEE, 65, 121 (1977).
5. G. L. Rogers: Noncoherent Optical Processing, John Wiley, New York, 1977.
6. E. N. Leith and J. Upatnieks, "Holography with Achromatic-Fringe Systems," J. Opt. Soc. Am., 57, 975 (1967).
7. R. E. Brooks, L. O. Weflinger, and R. F. Wuerker, "Pulsed Laser Holograms," IEEE, J. Quantum Electron., QE-2, 275 (1966).
8. S. Lowenthal and P. Chavel, in R. Wiener and J. Shamir, Eds., Proc. of ICO Jerusalem 1976, Conference on Holography and Optical Processing, Plenum Press, New York, 1977.
9. A. Lohmann, "Incoherent Optical Processing of Complex Data," Appl. Opt., 16, 261 (1977).
10. E. N. Leith and J. Roth, "White-Light Optical Processing and Holography," Appl. Opt. 16, 2565 (1977).
11. G. M. Morris and N. George, "Space and Wavelength Dependence of a Dispersion-Compensated Matched Filter," Appl. Opt., 19, 3843 (1980).
12. D. Gabor, "Laser Speckle and Its Elimination," IBM, J. Res. Develop., 14, 509 (1970).

13. F.T.S. Yu, Optical Information Processing, Wiley-Interscience, NY, 1983.

14. M. Born and E. Wolf: Principles of Optics, 2nd rev. ed., Pergamon Press, New York, 1964.

15. F.T.S. Yu, S. L. Zhuang, and S. T. Wu, "Source Erroding for Partially Coherent Optical Processing," Appl. Phys., B27, 99 (1982).

16. P. H. Van Cittert, "Die Wahrscheinlicke Schwingungs verteilung in einer von einer lichtquelle direkt Oden Mittels einer linse," Physica 1, 201 (1934).

17. F. Zernike, "The Concept of Degree of Coherence and Its Application to Optical Problems," Physica 5, 785 (1938).

18. F.T.S. Yu and S. T. Wu, "Color Image Contradiction with Extended Incoherent Source," J. Opt., 13, 183 (1982).

19. S. H. Lee, S. K. Yao, and A. G. Milnes, "Optical Image Synthesis (Complex Amplitude Addition and Subtraction) in Real-Time by a Diffraction-Grating Interfere Metric Method," J. Opt. Soc. Am., 60, 1037 (1970).

20. S. T. Wu and F.T.S. Yu, "Image Subtraction with Encoded Extended Incoherent Source," Appl. Opt., 20, 4082 (1981).

21. T. H. Chao, S. L. Zhuang, S. Z. Mao and F.T.S. Yu, "Broad Spectral Band Color Image Deblurring," Appl. Opt., 22, 1439 (1983).

22. F.T.S. Yu, K. B. Xu, T. N. Lin and T. H. Chao, "White-Light Optical Speech-Spectrogram Generation," J. Opt. Soc. Am., 72, 1722 (1982).

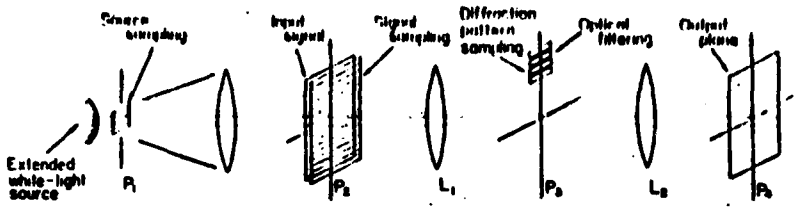


Figure 1. A white-light optical signal processor.

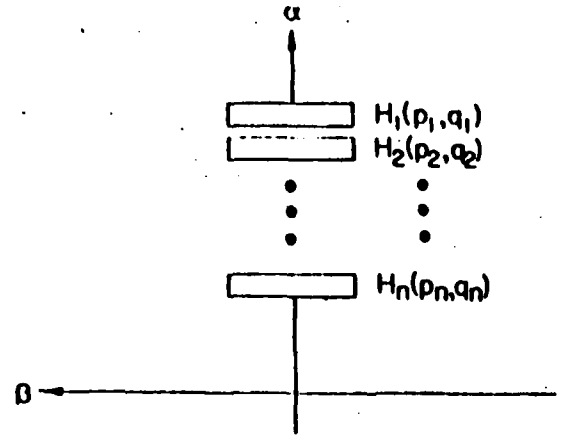


Figure 2(a). A multi spectral-band filter.

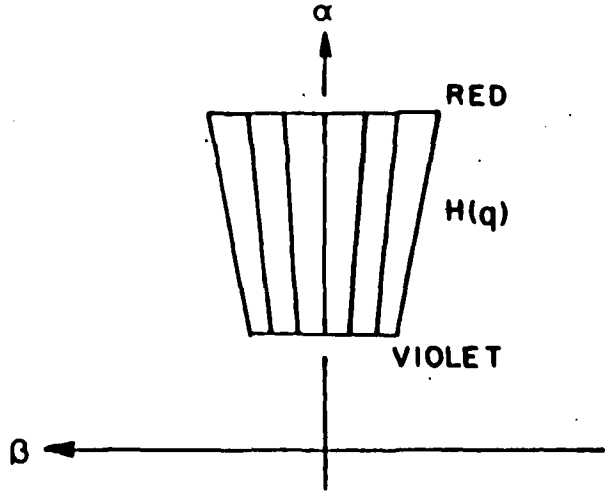


Figure 2(b). A fan-shape filter.

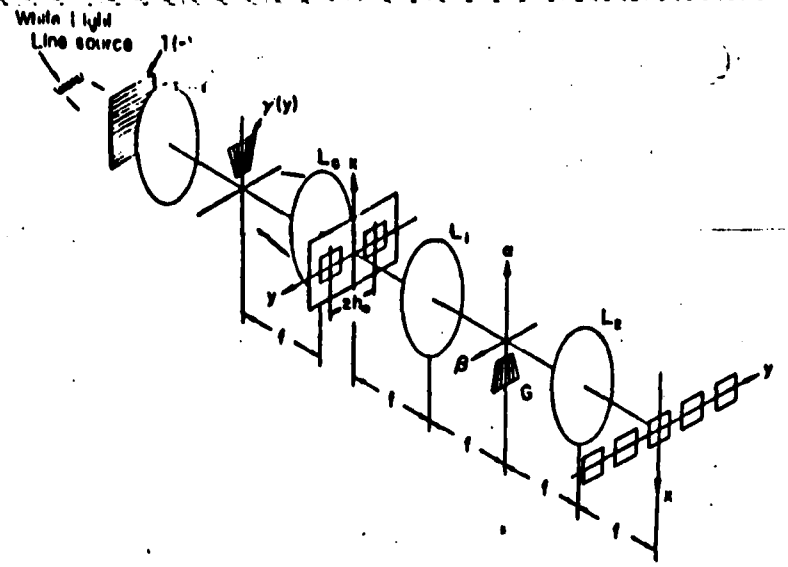


Figure 3. A white-light image subtraction processor. T(x); phase grating, $L_I$; image lens, $L_C$; collimated lens, $L_1$ and $L_2$; achromatic transform lenses, γ(y); source encoding mask, G; fan-shape diffraction grating.

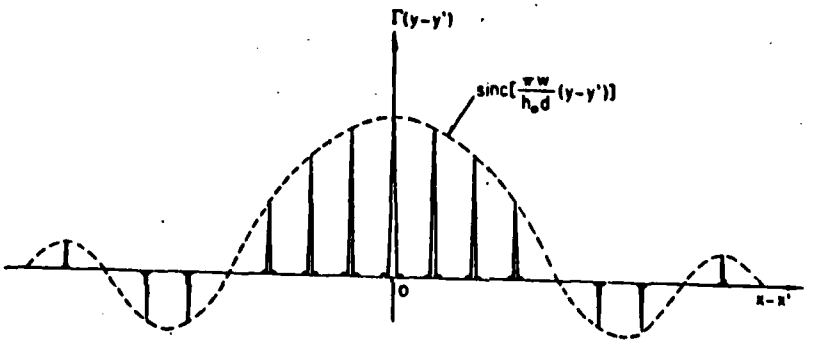


Figure 4(a). A spatial coherence function.

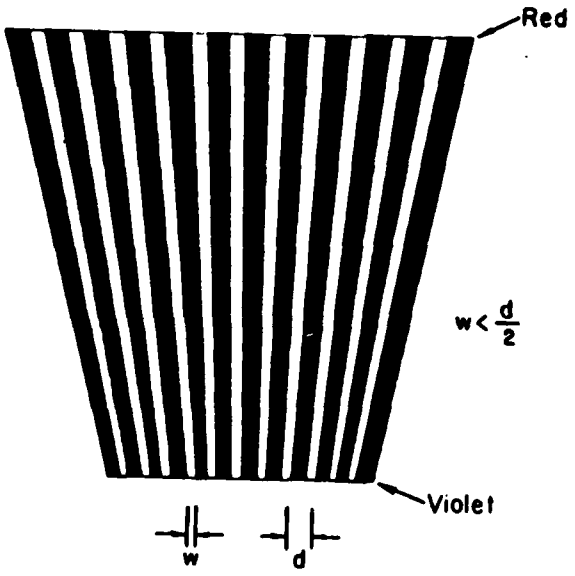


Figure 4(b). A source encoding mask.

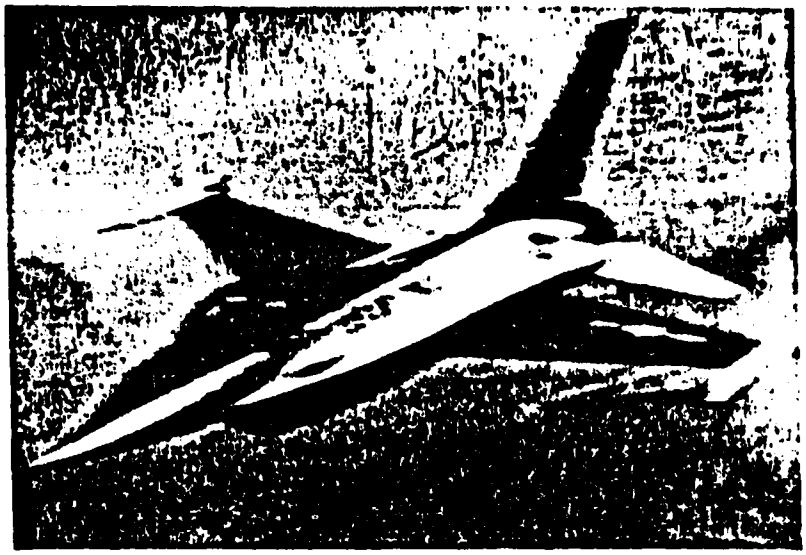

Figure 5(a). A black-and-white blurred color image.

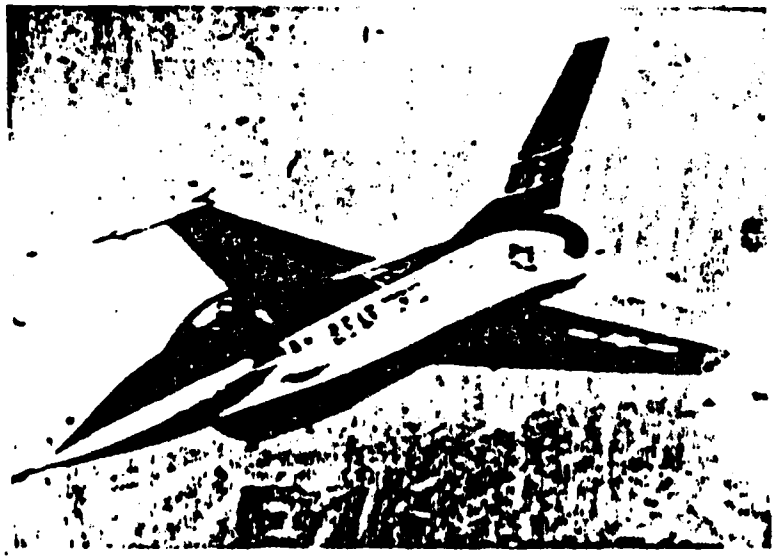

Figure 5(b). A black-and-white deblurred color image.

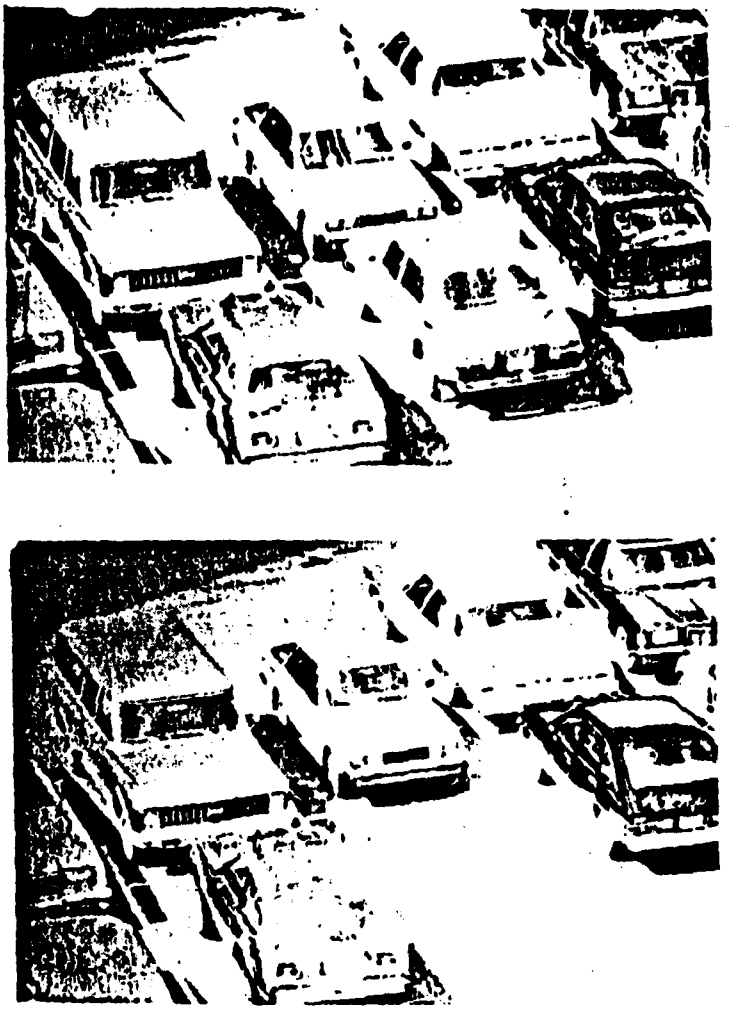

Figures 6(a) and (b). Black-and-white pictures of the input color objects.

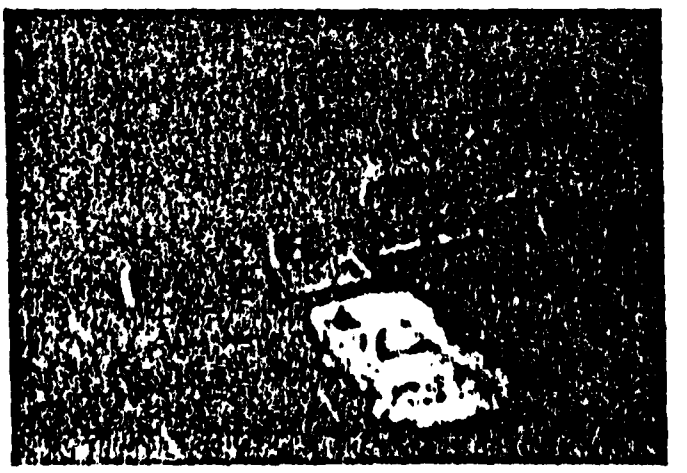

Figure 6(c). A black-and-white subtracted color image.

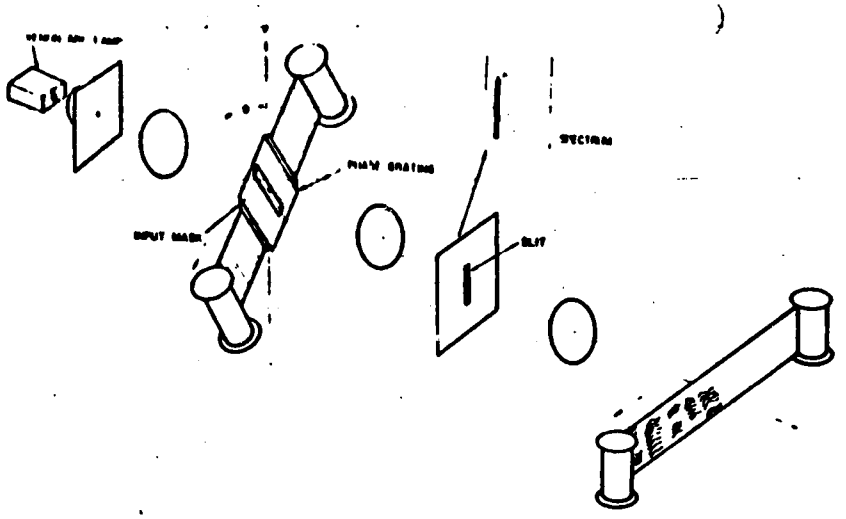


Figure 7. A white-light optical speech spectrograph.

Figure 8(a). An intensity modulated format.

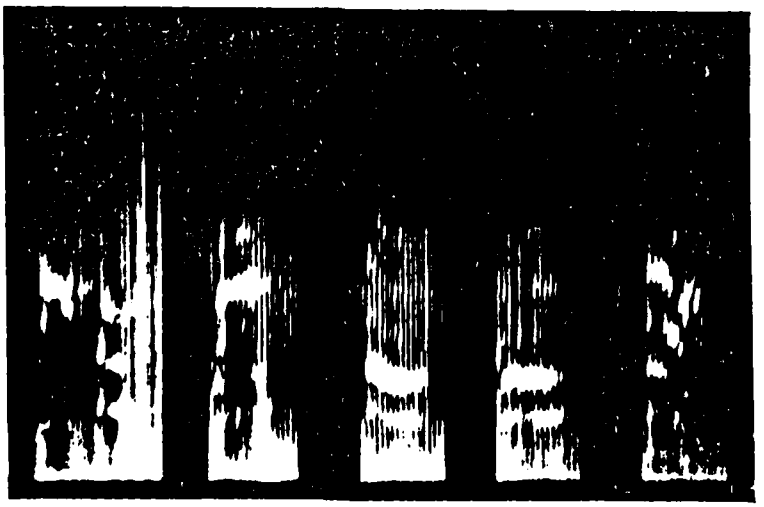

Figure 8(b). A black-and-white frequency color coded speech spectrogram. This spectrogram represents a sequence of English words "testing, one, two, three, four" spoken by a male voice.

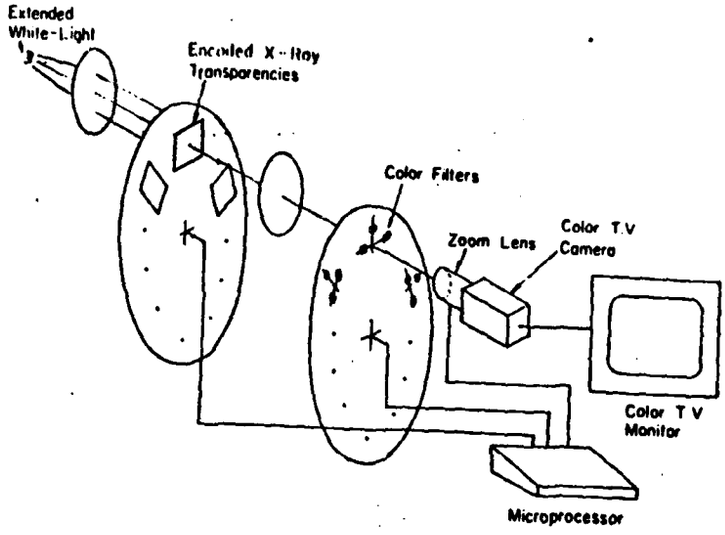


Figure 9. A computer controllable white-light density pseudocolor encoder.

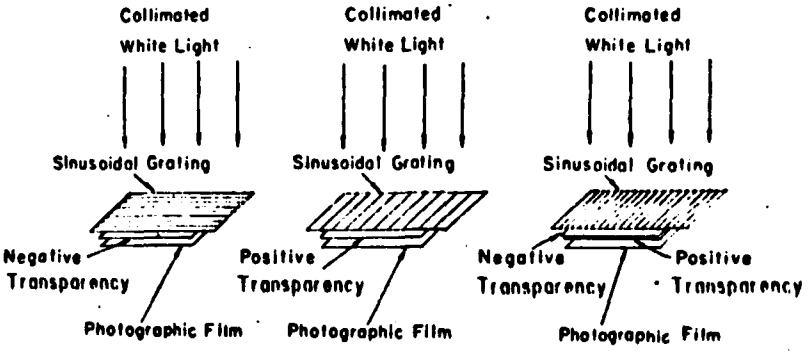


Figure 10. Spatial encoding.

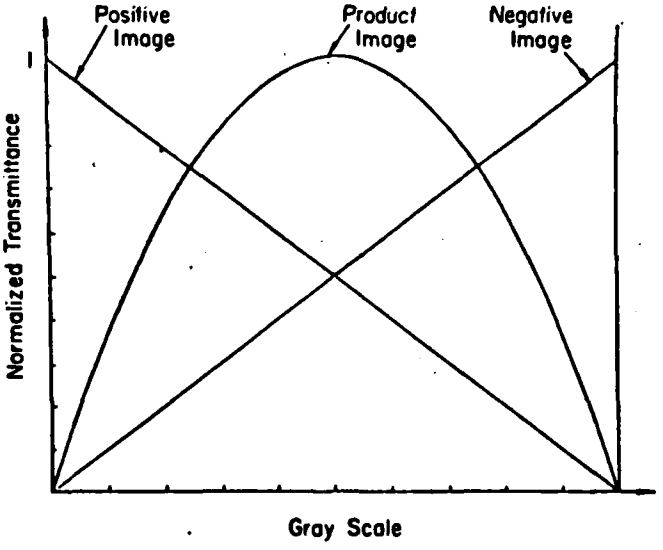


Figure 11. Normalized transmittance as a function of gray scale.

Fi

Figure 12(a). A black-and-white picture of a color coded picture. Positive image is encoded in red, negative image is encoded in blue, and product image is encoded in green.

Figure 12(b). A black-and-white picture of a reversal of primary color coded image of (b).

## IX. LIST OF PUBLICATIONS RESULTING FROM AFOSR SUPPORT


1. S. T. Wu and F. T. S. Yu, "Source Encoding for Image Subtraction," Optics Letters, Vol. 6, pp. 452-454, September, 1981.

2. F. T. S. Yu and J. L. Horner, "Optical Processing of Photographic Images," Optical Engineering, Vol. 20, pp. 666-676, September-October 1981.

3. F. T. S. Yu, "Partially Coherent Optical Processing of Images," SPIE Proceedings on "Processing Images and Data from Optical Sensors," Vol. 292, pp. 2-8, 1982.

4. F. T. S. Yu and J. L. Horner, "Review of Optical Processing of Images," SPIE Proceedings on Processing Images and Data from Optical Sensors," Vol. 292, pp. 9-24, 1982.

5. F. T. S. Yu, S. L. Zhuang and T. H. Chao, "Color Photographic-Image Deblurring by White-Light Processing Technique," Journal of Optics, Vol. 13, pp. 57-61, March-April, 1982.

6. S. T. Wu and F. T. S. Yu, "Image Subtraction with Encoded Extended Incoherent Source," Applied Optics, Vol. 20, pp. 4082-4088, December 1981.

7. F. T. S. Yu, S. L. Zhuang and S. T. Wu, "Source Encoding for Partial Coherent Optical Processing," Applied Physics, Vol. B27, pp. 99-104, February 1982.

8. S. T. Wu and F. T. S. Yu, "Visualization of Color Coded Phase Object Variation with Incoherent Optical Processing Technique," Journal of Optics, Vol. 13, pp. 111-114, May-June, 1982.

9. S. L. Zhuang and F. T. S. Yu, "Coherence Requirement for Partially Coherent Optical Information Processing," Applied Optics, Vol. 21, pp. 2587-2595, July 1982.

10. F. T. S. Yu and S. T. Wu, "Color Image Subtraction with Encoded Extended Incoherent Source," Journal of Optics, 13, 183 (1982).

11. S. L. Zhuang and F. T. S. Yu, "Apparent Transfer Function for Partially Coherent Optical Information Processing," Applied Physics, B28, 359-366, August, 1982.

12. Y. W. Zhang, W. G. Zhu, and F. T. S. Yu, "Rainbow Holographic Aberrations and Bandwidth Requirements," Applied Optics, 22, 164 (1983).

13. F. T. S. Yu, X. X. Chen, and S. L. Zhuang, "Progress Report on Archival Storage of Color Films with White-Light Processing Technique," submitted to Applied Optics.

14. T. H. Chao, S. L. Zhuang, S. Z. Mao and F. T. S. Yu, "Broad Spectral Band Color Image Deblurring," Applied Optics, 22, 1439 (1983).

15. F. T. S. Yu, Optical Information Processing, Wiley-Interscience, N.Y., 1983.

16. F. T. S. Yu, "Source Encoding, Signal Sampling and Filtering for White-Light Signal Processing," Proceedings of 10th International Optical Computer Conference, pp. 111-116, April 6-8, 1983.

17. X. J. Lu and F. T. S. Yu, "Restoration of Out-of-Focused Color Photographic Images," Optics Communications, Vol. 46, pp. 278-833, July (1983).

18. C. Warde, H. J. Caulfield, F. T. S. Yu and J. E. Ludman, "Real-Time Joint Spectral-Spatial Matched Filtering," Optics Communications, Vol. 49, pp. 241-244, March (1984).

19. F. T. S. Yu, "Source Encoding, Signal Sampling and Spectral Band Filtering for Partially Coherent Optical Signal Processing," Journal of Optics, Vol. 14, pp. 173-178, July-August (1983).

20. F. T. S. Yu, "Recent Advances in White-Light Optical Signal Processing," Conference on Laser and Electro-Optics, Cleo '83 Technical Digest, pp. 28-30, May (1983).

21. F. T. S. Yu, X. X. Chen and T. H. Chao, "Density Pseudocolor Encoding with Three Primary Colors," Journal of Optics, Vol. 15, pp. 55-58, March-April (1984).

22. F. T. S. Yu, S. L. Zhang and K. S. Shaik, "Noise Performance of a White-Light Optical Signal Processor: Part I, Temporally Partially Coherent Illumination, Journal of the Optical Society of America A, Vol. 1, pp. 489-494, May (1984).

23. F. T. S. Yu, F. K. Hsu and T. H. Chao, "Coherence Measurement of a Grating-Based White-Light Optical Signal Processor," Applied Optics, Vol. 23, pp. 333-340, January (1984).

24. F. T. S. Yu, "Advances in White-Light Optical Signal Processing," Proceedings on Optical Information Processing Conference II, NASA CP-2303 Conference publication, pp. 53-69, August (1983).

25. S. L. Zhuang, "Coherence Requirements, Transfer Functions and Noise Performance of a Partially Coherent Optical Processor," Ph.D. Dissertation, Pennsylvania State University, University Park, PA, 1983.

26. T. H. Chao, "A Grating-Based White-Light Optical Signal Processor," Ph.D. Dissertation, Pennsylvania State University, University Park, PA, 1983.

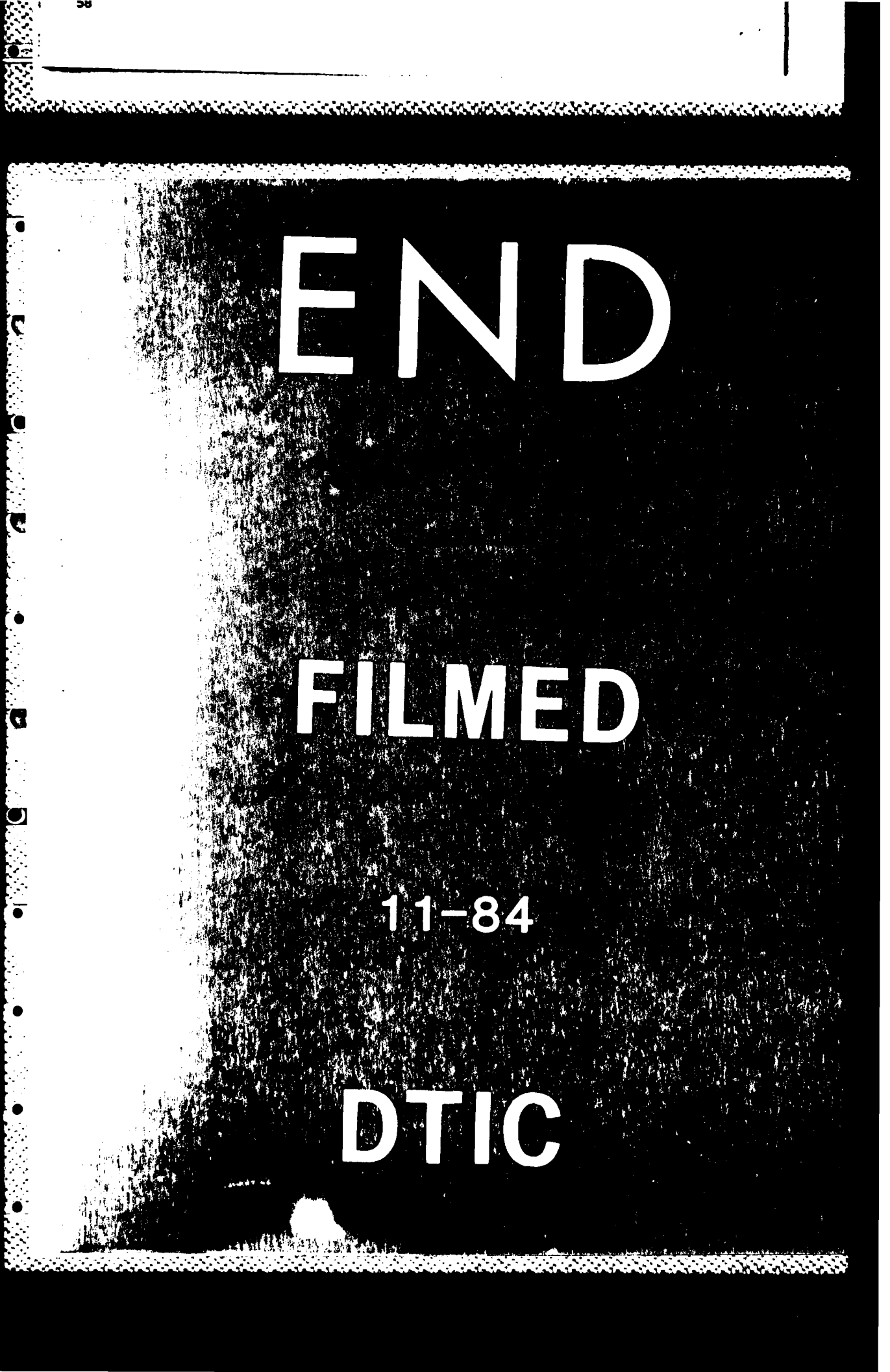
END
FILMED
11-84
DTIC